bioengineering

MDPI

Review

Technologies for Vitrification Based Cryopreservation

Mohammad Amini and James D. Benson *

Department of Biology, University of Saskatchewan, Saskatoon, SK S7N 5E2, Canada
* Correspondence: james.benson@usask.ca

Abstract: Cryopreservation is a unique and practical method to facilitate extended access to biological materials. Because of this, cryopreservation of cells, tissues, and organs is essential to modern medical science, including cancer cell therapy, tissue engineering, transplantation, reproductive technologies, and bio-banking. Among diverse cryopreservation methods, significant focus has been placed on vitrification due to low cost and reduced protocol time. However, several factors, including the intracellular ice formation that is suppressed in the conventional cryopreservation method, restrict the achievement of this method. To enhance the viability and functionality of biological samples after storage, a large number of cryoprotocols and cryodevices have been developed and studied. Recently, new technologies have been investigated by considering the physical and thermodynamic aspects of cryopreservation in heat and mass transfer. In this review, we first present an overview of the physiochemical aspects of freezing in cryopreservation. Secondly, we present and catalog classical and novel approaches that seek to capitalize on these physicochemical effects. We conclude with the perspective that interdisciplinary studies provide pieces of the cryopreservation puzzle to achieve sustainability in the biospecimen supply chain.

Keywords: cryobiology; physical chemistry; bioengineering; heat transfer; technology; vitrification

check for updates

Citation: Amini, M.; Benson, J.D. Technologies for Vitrification Based Cryopreservation. *Bioengineering* **2023**, *10*, 508. https://doi.org/10.3390/bioengineering10050508

Academic Editors: Haishui Huang, Xiaoming He and Elena A. Jones

Received: 24 January 2023
Revised: 8 March 2023
Accepted: 30 March 2023
Published: 23 April 2023

Copyright: © 2023 by the authors. Licensee MDPI, Basel, Switzerland. This article is an open access article distributed under the terms and conditions of the Creative Commons Attribution (CC BY) license (https://creativecommons.org/licenses/by/4.0/).

1. Introduction

Cryopreservation is one of the approaches to preserve cells and tissues over long time periods. Because of this, cryopreservation of cells and tissues is essential to modern medical science, including cancer cell therapy, tissue engineering, transplantation, reproductive technologies, and bio-banking. For example, one such application, liver cell transplantation (LCT), treats diseases involving liver metabolism [1–4]. In order to achieve sustainability in LCT, developing a liver cell bank of cryopreserved cells and tissues is critical to facilitate access to liver cells in clinical centers [5]. In 2017, 23.3% of all organ transplantations were liver transplants (32,348 transplanted livers) [6]. Although these numbers are high, the actual number of liver donors was much higher, i.e., 27% of donors' livers were not transplanted due to limitations, resulting in many patients dying whilst on the waiting list. Early cancer therapy has improved the survival rates of women who need to cryopreserve their ovarian tissue due to gonadotoxic treatment [7]. Cryopreservation is also a vital part of the supply chain of new cell sources for regenerative medicine [8]. In response to climate change and global warming, a wide range of cells and tissues must be cryopreserved for both plant and animal species conservation [9–11]. Finally, rapid freezing methods have many advantages in histological applications compared to chemical preservation, such as chemical fixation applicable in electron microscopy [12].

Cryopreservation often results in significantly reduced cell and tissue viability due to ice crystal formation. This reduced viability is attributed to several classes of damage, including osmotically induced volume changes [13], damaging ice formation [6], cytosol concentration changes [14], and thermal stress due to cooling and warming [15]. Water solidifies as ice at low and moderate cooling rates and can form deleterious intra- and inter-cellular ice crystals [16]. During this gradual solidification, the extracellular media becomes divided into two parts. The first part is ice, generally considered pure water

because ice cannot dissolve significant amounts of solutes. The second part is unfrozen water, which dissolves the remaining solutes. Therefore, the concentration of the solution increases gradually as the ice grows. This high solution concentration is considered to be a toxic cell environment [17].

Chemical and biological materials, called cryoprotectant agents (CPAs), have been crucial in decreasing damage due to ice formation and excessive ion concentrations. However, a high concentration of CPAs harms cells and tissues because it leads to cellular osmotic and mechanical stress as the result of volume changes (shrinking and swelling) during the addition and removal of CPA. In addition, biophysical and biochemical interactions between CPA and cytoplasmic constituents cause toxic effects in a biological sample [13,18–23].

One approach to avoid damage due to ice formation is to use ice-free cryopreservation, known as vitrification, to reduce the potential toxicity of high solute concentrations below 0 °C and avoid ice crystallization and growth. There is a non-crystalline state at extremely low temperatures in which cells and tissues are considered safe. This state is called a glassy or vitreous state, and the material forming in this state is called glass. A sufficiently concentrated solution can vitrify at any cooling rate [24], but these high concentrations are associated with significant toxicity. However, due to the formation of hydrogen bonds between water molecules, ice crystallization is a time-dependent phenomenon. Therefore, to avoid crystal formation and achieve a vitreous state under less toxic CPA concentrations, it is necessary to pass through the related states of heterogeneous and homogeneous ice formation as quickly as possible (Figure 1). The minimum cooling rate to vitrify pure water was estimated on the order of 10^8 °C/min [25], not achievable for droplets with diameters more than 10 µm [26]. However, cells seemingly can tolerate ice crystals with dimensions less than 1 µm [27]. Hence, CPA-free cell cryopreservation has been carried out in droplets with a maximum volume of 200 pL, equivalent to a sphere of diameter 70 µm [26]. Therefore, it is generally desirable in "vitrification protocols" to cool and warm samples as rapidly as possible without causing damaging thermal stress.

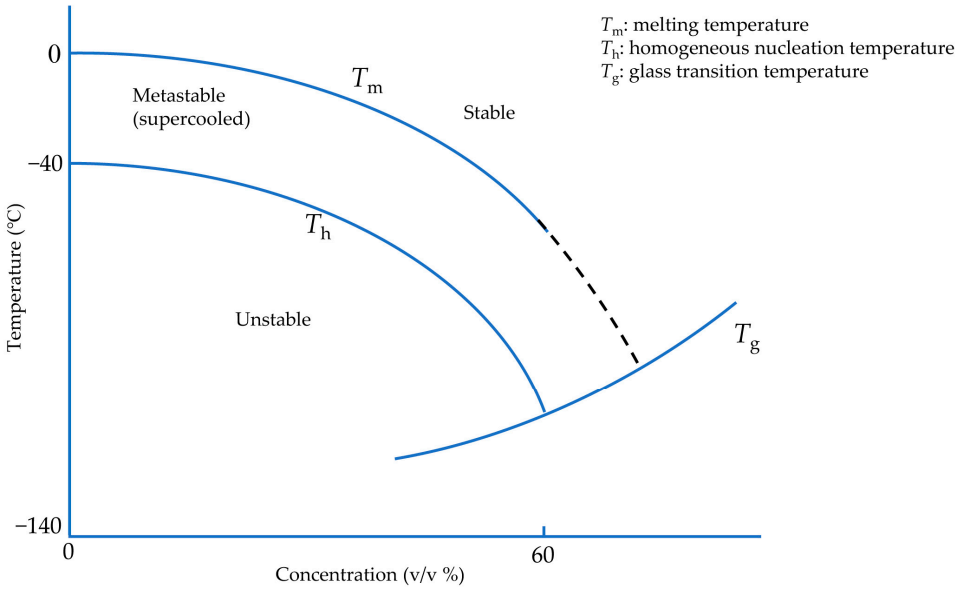

Figure 1. Idealized and modified phase diagram of CPA-water solution during vitrification. Adapted with permission from Ref. [24], 2023, Elsevier.

To achieve rapid cooling rates there have been two primary methods to reach vitrification: moving a cryogen over the sample (convection method) and using solid surface cooling (conduction method) [28]. The convection method is generally limited by the Leidenfrost effect: when a biological sample directly contacts a cryogen such as liquid nitrogen, the large temperature difference creates a vapor film between the sample and the cryogen. This film acts as an insulating layer around the biological sample, resulting in

reduced heat transfer coefficients and, thus, dramatically reduced cooling rates in the biological sample [29]. However, in solid surface cooling, the sample contacts a cooled surface with high thermal conductivity and diffusivity to maintain the temperature gradient. This method can avoid the Leidenfrost effect due to indirect contact between the sample and cryogen [28]. Another approach to reducing the required CPA concentration is to apply hydrostatic pressure because the glass transition temperature can be increased by hydrostatic pressure [30]. In addition, with increasing hydrostatic pressure, the melting point of water reduces [31–33]. Therefore, high hydrostatic pressure can reduce the temperature difference between the melting point and the glass transition temperature. In short, with or without the increase of pressure, the goal of vitrification in each of these methods is to pass through this temperature range at a high cooling rate, preventing large ice crystals formation or growth (Figure 1) [34].

Each approach is associated with significant hurdles, including contamination due to direct contact between biospecimen and liquid nitrogen [35] and the Leidenfrost effect [30]. Moreover, most solid surface devices cool a sample from just one side. Consequently, cooling depth reduces, and satisfactory survival depth is not achievable [16]. Therefore, the usual tradeoff is that immersion in a cryogen removes heat from all sides but encounters reduced cooling rates, and solid surface cooling removes heat faster, but only from one side. An apparatus that can use solid surfaces to cool a contained biospecimen from two sides and reduce CPA concentration by applying a high cooling rate could partially address this dilemma [16].

In this review, we discuss the physical chemistry of cryopreservation and, specifically, vitrification. Further, we explore the effect of hydrostatic pressure in vitrification and on biological samples. Finally, a number of methods, technologies, and devices used in vitrification are presented, and results are summarized.

2. Physical Chemistry Aspects of Vitrification

2.1. Vitrification

As pure liquid water is cooled below its melting temperature (T_m), it first passes into a region called the supercooled liquid state, as shown in Figure 1 [36]. In this region, water molecules combine to form a cluster due to Brownian motion as a base for ice nuclei formation [17]. Based on classical nucleation theory [37], water below melting temperature is in a metastable state corresponding to a minimum of the appropriate thermodynamic potential without any crystal formation [38]. If, by stochastic fluctuations, an ice-aggregate of a sufficiently large size is formed, known as critical cluster, it can further grow in accordance with thermodynamic evolution laws. The radius of the critical cluster has quite different values depending on pressure and temperature. It tends to infinity, near the melting temperature. At the radius of the critical cluster, more water molecules favor thermodynamically binding the critical cluster and making it larger. Afterward, this critical cluster may enable the entire supercooled liquid to experience a significant phase transition, known as freezing.

The number of critical clusters per unit of volume in a specific temperature can be calculated thermodynamically. Ice critical cluster formation in the aqueous solution necessitates an entropy decrease and maybe creates a barrier against nucleation. The energy barrier is the result of the related change in Gibbs energy to create the critical cluster containing a number of water molecules. Therefore, the energy barrier must be conquered to form the ice critical cluster. The energy barrier includes a volume term and a surface term. The volume term is related to the chemical potential decrease of the critical cluster with respect to the supercooled state due to phase change. The surface term is related to the energy required to create the critical clusters interface.

Although liquid water can be prolonged in the supercooled state, homogeneous nucleation may occur at any temperature below melting temperature (T_m) with a highly different probability. Homogeneous nucleation temperature (T_h) is where homogeneous nucleation becomes increasingly probable [39]. A maximum nucleation rate exists depending on the

temperature, occurring near the conventional glass transition temperature (T_g), at which a glassy or vitreous state of non-crystalline material can form [40]. This transition is not associated with a specific temperature where the vitreous state forms but rather a temperature interval at which the process takes place. On the other hand, water impurities and container surfaces can contribute to heterogeneous ice nucleation earlier in supercooled water due to the energy barrier deduction of heterogeneous nucleation compared to homogeneous nucleation [41].

However, if the cooling rate is sufficiently high, these ice nuclei do not have sufficient time to grow due to water molecule diffusion limitations. By including a cryoprotectant agent (CPA), the medium viscosity increases [42], facilitating an ice-free medium, or at least a medium with only tiny ice crystals, known as the "non-harmful" ice crystals, which can be achieved in the supercooled region and below T_m without substantial ice crystal growth. This kind of ice crystal is too small to be seen by an electron microscope [28]. On the other hand, because of an insufficient cooling rate due to the thickness of the biological sample or the volume of the medium, "harmful" ice crystals can form and be seen by the electron microscope since there is enough time and energy for water molecules to develop ice crystal nuclei [43]. To sum up, after cryoprotectant toxicity, the most influential factor that influences cell and tissue viability is ice crystal size.

In glasses, the values of thermodynamic response variables, such as the specific heat and coefficient of expansion, are closer to those of the crystalline form than to the liquid state [40] (Figure 2). In contrast, x-ray diffraction studies show that the structure of glasses, such as silicate glasses [44,45], resembles the structure of their liquid form. In fact, the enthalpy, entropy, and specific volume of the glass are the same as those for liquids, which is why there is no latent heat in the transition of glass formation [40]. On the other hand, the rate of change of these thermodynamic state variables is close to those of the crystalline form. This is mainly because glass is a form of liquid with high viscosity. In a method reported in the literature, Boutron [46–49] and others [50–53] measure the glass transition temperature (T_g) based on a sudden change in heat capacity using a differential scanning calorimeter (DSC) [24].

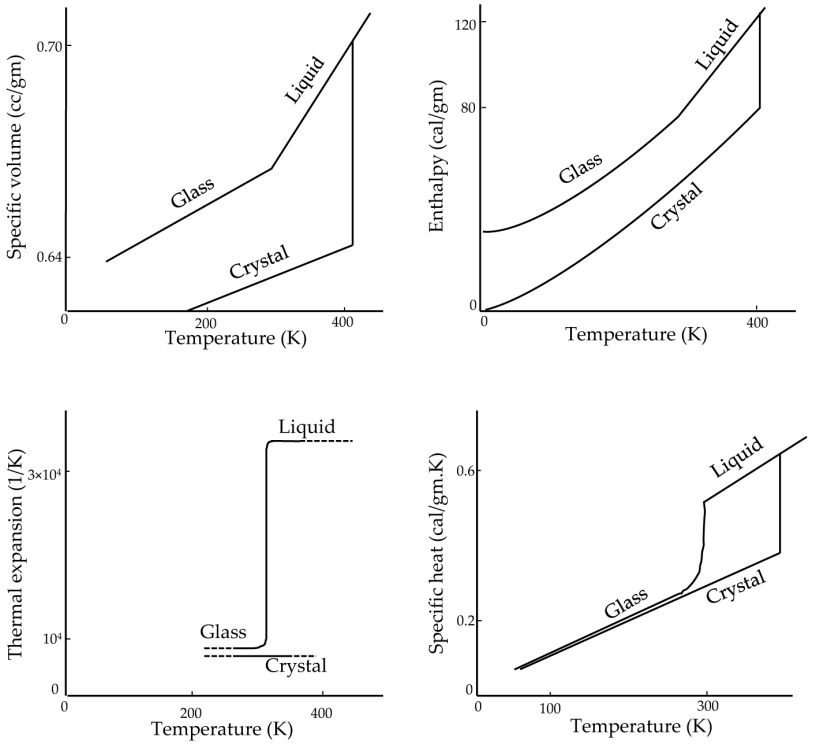

Figure 2. Thermodynamic properties of glucose. Adapted with permission from Ref. [40], 2023, American Chemical Society.

2.2. High Hydrostatic Pressure

Due to the influence of high hydrostatic pressure on reducing the melting temperature and increasing the glass transition temperature, the application of high hydrostatic pressure towards preserving biological systems commenced in the 1970s to reduce ice damage during freezing [54]. This technique has been widely used for biospecimen fixation with applications in electron microscopy [55,56]. However, there are few studies of cryopreservation of living cells and tissues under hydrostatic pressure and ultra-rapid cooling, and further studies are required to investigate living specimens during cryopreservation [57].

Under ambient pressure, water freezes in a hexagonal form known as Ice I [31]. As shown in Figure 3, by increasing the hydrostatic pressure, the melting temperature of water reduces. This process continues until about 205 MPa (2050 bar), where Ice II or Ice III form high-pressure shapes of ice. After this point, with increasing pressure, the melting temperature of high-density configurations of ice increases. Therefore, the minimum melting temperature of the water is −23 °C (250 K) under 205 MPa pressure. Moreover, pressure can influence water viscosity, resulting in an increase in the glass transition temperature [30]. In this way, and similar to the concentration of solutes, decreasing the melting temperature and increasing the glass transition temperature, the high hydrostatic pressure may improve vitrification.

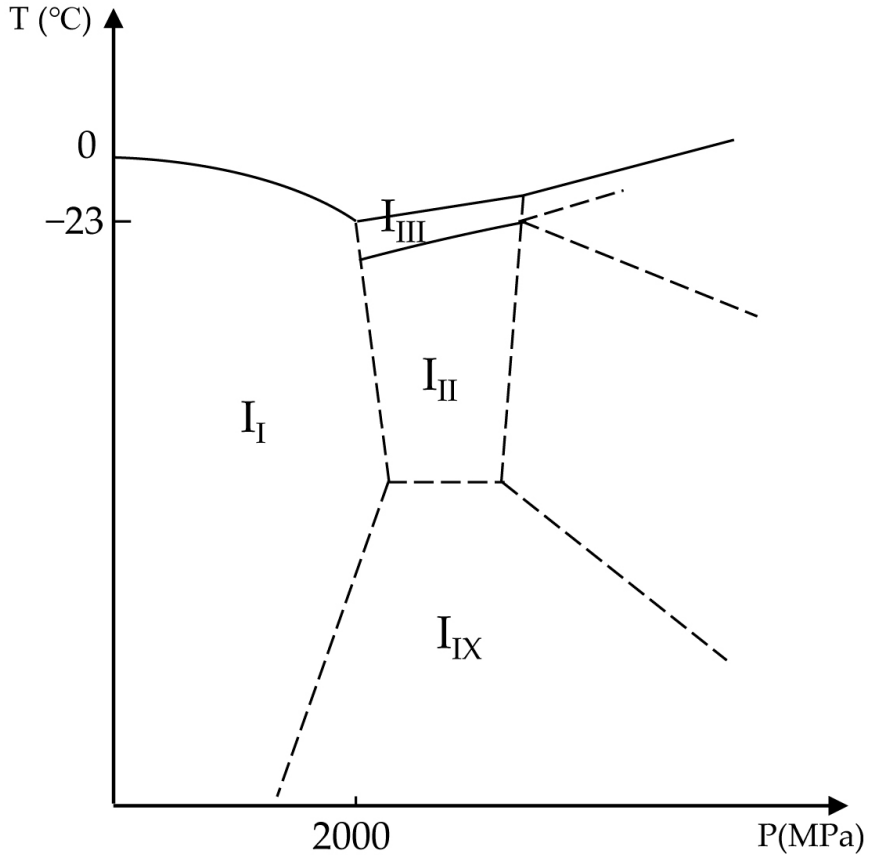

Figure 3. Phase diagram of ice as a function of temperature and pressure. I_I, I_{II}, I_{III}, and I_{IX} are ice shapes of Ice I, Ice II, Ice III, and Ice IX, respectively. Adapted with permission from Ref. [31], 2023, Elsevier.

To establish a theoretical foundation for further experimental designs, Miyata et al. investigated the vitrification of aqueous glycerol solutions under high pressures at low cooling rates (3 °C/min) [30]. Miyata et al. observed that the temperature corresponding to the maximum homogeneous nucleation rate decreased with increasing pressure up to about 200 MPa, and after that, this temperature increased with pressure. In contrast, the

glass transition temperature (T_g) increased linearly with pressure, but the slope decreased as solution concentration decreased and would be zero for pure water.

At atmospheric pressure, water is less viscous. Therefore, as the ice grows in the medium, additional water molecules are recruited to make larger ice crystals. However, under high pressure, water becomes much more viscous. Consequently, the growth rate of ice crystals is reduced by high pressure. At atmospheric pressure, freezing causes ice crystals with rough surfaces, resulting in mechanical injury to the membrane of cells and tissues [58]. On the other hand, the surface of ice crystals at high pressure is much smoother and could possibly cause less mechanical damage to the cell membrane [59]. One advantage of applying high pressures in cryopreservation is the potential to reduce or eliminate ice crystal formation in much deeper regions inside a biological sample [19]. In cryomicroscopy, where the preservation of ultrastructure is paramount and post-thaw viability is not a priority, Sartori et al. found they could increase the vitrification depth more than 10-fold by applying high pressure during freezing [60]. Heuser and Staehelin [28] claimed that it would be possible to vitrify up to the depth of 600 μm in planar samples and 1 mm in spherical samples by high pressure in comparison with the 40 μm depths that was achieved at atmospheric pressure.

2.3. Warming

Recrystallization is defined as the growth of ice crystals in the warming process [24]. Ice nucleation happens rapidly at lower temperatures due to the low free energy barrier. In fact, the vitrified solution can transform into ice crystals at temperatures higher than T_g due to the metastability of the solution with respect to ice formation. This nucleation forms a base for extensive ice crystal growth at higher solution temperatures. For example, the peak of the ice nucleation rate occurs around T_g, and ice nucleation even happens at temperatures lower than T_g. This is because in order to form ice nuclei, local replacement of molecules is all that is needed [61]. However, ice growth occurs at higher temperatures. At lower temperatures, the solution is more viscous, which limits the diffusion of water molecules to the crystal clusters. On the other hand, in dilute solutions, there are regions in which ice nucleation and growth overlap with a broader range [62] because water molecules share hydrogen bonds with each other rather than with solute molecules and are, therefore, able to participate in ice crystal growth at lower temperatures. In this regard, the warming rate that significantly prohibits ice crystal formation and growth during warming is called the "critical warming rate" [46]. Tiny ice crystals are highly likely to be formed in ultra-rapid freezing. However, cells can seemingly survive the presence of tiny ice crystals [63–66]. This is where the warming rate can play a significant role. At slow warming rates, the vitrified solution recrystallizes and forms large ice crystals, damaging cells [63,64]. For example, Mazur et al. [67] cryopreserved Chinese hamster cells by fast freezing coupled with ultrafast warming—clearly, adding heat energy is simpler than removing it. These cells had higher survival compared with those cryopreserved at the slow freezing rate. The authors claimed that one reason could be the lower salt concentration due to lower cell dehydration associated with rapid freezing. However, by slow warming, de Graaf and Koster [68] reported low viability in rapidly frozen rat liver slices. By DSC technique, Amini and Benson [69] show that, under ultra-rapid freezing, ice recrystallization does not happen in low CPA concentrations during slow warming; however, in moderate and high CPA concentrations, ice recrystallization is a dominant part of ice formation in slow warming.

In some references, the temperature related to crystallization in the warming process is called recrystallization temperature (T_r) [28,42,70]. In a solution with high molecular weight solutes, T_r is recorded at higher temperatures. This T_r has practical implications: Bank [71] rapidly warmed yeast cells from liquid nitrogen and at −50 °C in the duration of 24 hr did not observe any ice crystal damage under the condition of CPA-free. However, Bank reported visible ice crystals at −45 °C after 30 min and at −20 °C after just 5 min. There was massive damage inside the cells.

Rall et al. [72] mentioned that T_r is −50 °C for mouse embryos. Gilkey and Staehelin [28] did not observe any recrystallization in the range of −95 and −50 °C in a large number of samples and under CPA-free conditions. In the case of CPA-free vitrification, it seems that T_r is reduced. For example, a CPA-free suspension of red blood cells has T_r of −30 °C, while T_r is −80 °C for this suspension with 30% glycerol [73].

3. Biological Aspects of Cryopreservation

3.1. Cryopreservation of Isolated Cells and Tissue Slices by the Method of Vitrification

Cryopreservation facilitates the nearly indefinite storage of cells and tissues in a state of biological arrest [74]. The temperature of storage is critical: proteases are still active in the range from −20 °C to −80 °C, and between −80 °C and −130 °C, ice crystal formation is most likely due to the high homogeneous nucleation rates. Thus, the storage of biological samples is limited at these temperatures, but below −130 °C, there is no usable thermal energy for biochemical reactions [5]. Because of the massive shift in thermodynamic properties at the glass transition temperature and because the minimal T_g of water/CPA systems is around −140 °C, this is considered the maximal safe temperature for long-term storage of cryopreserved cells and tissues [75–78].

Generally, a cell and tissue "bank" is a collection of cryopreserved cells and tissues [68] that can be warmed as the needs arise. In fact, Luyet performed the first vitrification in 1937 [79], and the first success in live human birth by vitrified sperm was in 1953 [80]. Vitrification of liver slices (human) was attempted by Wishnies et al. in a highly concentrated solution of 4.7 mol/L 1,2-propanediol [81]. They placed nylon mesh containing slices into the liquid nitrogen directly with an estimated cooling rate of 5000 °C/min, and after warming, reached the high inherent biotransformation rate compared to fresh slices.

Different approaches have improved the vitrification of precision-cut liver slices (PCLS). For example, de Kanter and Koster [82] showed that by stepwise CPA addition (where the final concentration is reached after intermediate steps), they were able to improve the viability of rat liver slices when they used rapid freezing (250 °C/min) and 12% DMSO. Similarly, de Kanter et al. [83] claimed that human liver slices cryopreserved successfully by rapid freezing had 66% viability compared with fresh slices. de Graaf et al. [84] found that increasing DMSO concentration to 18% in pre-incubation before freezing could enhance some viability metrics.

Another approach for improving rapid freezing in PCLS was using a high thermal conductivity material such as aluminum plates in the freezing and thawing process [85]. In this method, the samples are placed between aluminum plates separated by a gasket and submerged in liquid nitrogen. This is why a higher cooling rate in the cryopreservation of liver tissues is crucial compared to isolated rat hepatocytes [86–89]. This can be explained by the difference between the structure of isolated cells and tissue slices as a group of cells together. In isolated cells, the extracellular ice crystals do not damage the cells; however, ice crystals accumulated between the cells in tissue slices can injure the cell and tissue structure [90,91]. In contrast to slow freezing, extracellular ice crystals do not form significantly during successfully implemented rapid freezing.

The cytoplasm tends to vitrify more readily than the extracellular medium because of the high concentration of intracellular proteins [92,93]. Furthermore, due to the structure of cells and tissue, water is not homogenously distributed and is divided into smaller portions. This water discontinuity in the intracellular and intercellular spaces can postpone the formation of ice crystals because, by decreasing the volume, the probability of ice formation reduces [94,95]. Therefore, lower concentrations of CPA are required to achieve vitrification inside cells and tissues compared to the extracellular/extra-tissue solutions. According to these concepts, de Kanter and Koster [82] postulated that during rapid freezing, water vitrifies inside the slices and forms ice crystals outside the slices, and they suggest that cells in the inner layer of slices can be protected by outer layers exposed to ice crystals formed in the medium.

Several sample-containing devices, or cryocarriers, designed to facilitate vitrification have been developed, including cryoloop, straw (and many variations thereof), Cryotip, Cryopette, VitriSafe, S3 μS-VTF, S3 system, Rapid-i [96–99]. These cryocarriers have seen considerable success but have a number of limitations. To wit, because the cooling rate is dependent on the sample volume, the cooling rate is reduced, especially in the interior part of the sample, due to thermal diffusivity, and this necessitates higher CPA concentrations to avoid ice crystals at the center of the tissue and decreases the viability of the sample [100–102]. Because of this, most vitrification cryocarriers are tailored to very small volume samples (<0.1 μL), which means applications to all but the smallest tissues (e.g., no larger than embryos) are precluded. Additionally, while these commercially available cryocarriers achieve high heat transfer, they are still usually limited by the Leidenfrost effect, which reduces the heat transfer between the sample and liquid nitrogen [29,103,104]. Finally, one pressing issue in using open vitrification carriers, which do not entirely cover the biospecimen, is contamination due to the sample's direct contact with liquid nitrogen associated with disease transfer to and from the samples [105–118].

Table 1 presents a number of cryopreserved samples, cryocarriers, and outcomes using the vitrification method.

Table 1. Cell and tissue slice cryopreservation by vitrification.

Sample	CPA Solution	Cryocarrier	Sample Size	Viability Evaluation	Outcome	Ref.
Ovine embryo	15% EG + 15% DMSO + 0.5 M sucrose + 30% Ficoll 70	Cryotop-Spatula	<0.1 µL	Embryo morphology Cell membrane integrity with propidium iodide	79.7% viability	[119]
Cow blastocyst	16% EG + 16% DMSO + 0.5 M sucrose	Fork	0.5 µl	Immunostaining	74% hatching rate with warming in straw	[120]
Donkey embryo	15% EG + 15% DMSO + 0.5 M sucrose + 18% Ficoll 70	Cryotop	<1 µL	Transrectal ultrasonography to track follicular activity and confirm ovulation Cell membrane integrity with propidium iodide and Hoechst 33342	70% viability	[121]
Bovine oocytes	2% EG + 2% PG	Cryotop	<1 µL	Oocyte viability, nuclear maturation status, embryo development, and blastocyst quality	15% blastocyst yield	[122]
Mouse embryo	20% EG + 0.4 M sucrose + 24% Ficoll 70	Cryotube	5 µL drop	Developmental ability	98.7% viability	[123]
Human ovarian tissue	30% EG + 0.5% trehalose + 6% FBS	Cold solid-surface, Straw, drop size into LN_2	100 µL	Histologic analysis	Higher morphological follicles by the method of drop size into LN_2	[124]
Ovine cumulus-oocyte complexes	VS1, VS2	Plastic insemination straw	250 µL	Morphological evaluation, Trypan blue staining	54.5% viability, 16.8% ultrastructural changes	[125]
Bovine oocyte	15% EG + 15% DMSO + 1.0 M sucrose	Hollow fiber	Inner diameter 200 µm, wall thickness 15 µm	Acetolacmoid staining	23% blastocyst yield	[126]
Human embryo	15% EG + 15% DMSO + 0.5 M sucrose	Plastic blade	Thickness: 0.05 mm	Assessment of pregnancy by transvaginal ultrasound imaging	100% viability in Blastocyst	[127]
Bovine oocytes	7.5% EG + 7.5% DMSO	Silk fibroin sheet multilayer	0.1 mm thickness, 0.7 mm width, 10 mm depth	Morphological survival rates	23% blastocyst yield	[128]
Rabbit chondrocyte sheets	20% EG + 20% DMSO + 0.5 M sucrose + 10% COOH-PLL	Sealable polyethylene bag and nylon meshes	110 × 85 mm; film thickness: 0.063–0.064 mm	Trypan blue staining Histological examination Immunohistochemical staining	91% viability	[129]

Table 1. *Cont.*

Sample	CPA Solution	Cryocarrier	Sample Size	Viability Evaluation	Outcome	Ref.
Human liver tissue	4.7 M 1,2-propanediol	Honeycomb-like tray	Diameter: 1 cm, Thickness: 200–250 µm	Xenobiotics metabolism	7-EC metabolism, 7-HC conjugation (Results are very unstable)	[81]
Human ovarian tissue	7.5% EG + 7.5% DMSO + 20% FBS + 13.5% EG + 13.5% DMSO + 0.5 mol/l sucrose	Needle directly into LN_2	1 mm^3	Histologic Analysis by H&E Ultrastructural evaluation using TEM TUNEL assay for detection of apoptosis Assessment of tissue damage using an LDH assay	Higher viability in stroma cells and lower apoptotic primordial follicles	[130]
Human ovarian tissue	10% DMSO + 10% EG	Direct cover vitrification (DCV)	1 × 1 × 1 mm	Follicle examination using electron microscopy and TUNEL	Higher normal follicles and lower apoptotic cells	[131]
Ovine testicular tissues	18% EG + 18% DMSO + 0.5 M trehalose	E. Vit (modified plastic straw)	1 mm^3	Cell plasma membrane integrity	73.6% viability	[132]
Human ovarian tissue	2.62 mol/L DMSO + 2.6 mol/L acetamide + 1.31 mol/L PROH + 0.0075 mol/L PEG	20 µL droplet into LN_2	4 mm × 4 mm × 1.5 mm	Immunohistochemistry histology	Higher follicles growth	[133]
Cat testicular tissues	15% EG + 20% glycerol + 0.5 M sucrose	Needle	1–2 mm^3	Seminiferous tubule Morphology Mitochondrial activity Cell composition	92.9% viability	[134]
Human ovarian tissue	40% EG + 1 M sucrose + 30% ficoll 70	Cryovial	2 mm^3	Histological examination Molecular assessment Hormonal assay Immunocytochemistry	95.5% viability	[135]
Mouse testicular tissues	15% EG + 15% DMSO + 0.5 M sucrose	Metal grid	Tissue fragments (0.5–1 mm^2)	Trypan blue staining Hematoxylin and eosin (H&E) staining Immunohistochemistry staining	97.7% viability	[136]

Table 1. *Cont.*

Sample	CPA Solution	Cryocarrier	Sample Size	Viability Evaluation	Outcome	Ref.
Dog ovarian tissue	15% EG + 7.5% DMSO + 0.5 M sucrose + 2.5% PVP	Needle	Diameter: 2 mm	Neutral red staining Histology Xenotransplantation assays	94.5% follicular viability	[137]
Rat testicular tissues	15% EG + 15% DMSO + 0.5 M sucrose	Inoculation loop	Pieces of approximately 3 mm	Trypan blue staining histological evaluation	84.8% viability	[138]
Rabbit trachea	18% EG + 22% DMSO + 0.5 M sucrose	Cryotube	0.5 cm × 0.5 cm	Morphological and ultrastructural assessment HE examination TUNEL assays TEM and SEM	97% viability	[139]
Rat kidney tissue	VM3 (8.44 M) in VS4 buffer (7.5 M)	Cryovial	Diameter: 5 mm	ATP content Histological integrity	Cortex: histomorphology (86%), ATP content (113%); medulla: histomorphology (79%), ATP content (68%)	[140]
Rat liver tissue	VM3 (8.44 M) in VS4 buffer (7.5 M)	Cryovial	Diameter: 8 mm	ATP content Histological integrity	histomorphology (71%), ATP content (58%)	[140]
Human osteochondral dowel	9.5% EG + 18% DMSO + 5.8% PG + 14.1% glycerol + 0.1 mg/mL chondroitin sulfate (CS)	5 mL vial	Full thickness in 10 mm diameter	Membrane integrity Metabolic activity Histology Immunohistochemistry	75.4% viability	[141]
Pig osteochondral dowel	16.6% EG + 21.5% DMSO + 22% PG + 0.1 mg/mL CS	Conical tube	two diameter sizes (10.0 mm and 6.9 mm) with 10 mm thickness	Chondrocyte assessment with membrane integrity stain and the chondrocyte metabolic activity by Alamar Blue.	60–80% viability	[142]

VM3 and VS4 are commercial CPA, consisting of buffer components such as NaCl, $NaHCO_3$, KCl, . . . , and CPAs such as DMSO, Formamide, and Ethylene glycol.

3.2. Effect of Hydrostatic Pressure on Biological Samples

Pressure, similar to temperature, is a thermodynamic parameter that can affect any thermodynamic system, such as biomolecular media. In nature, the range of pressure that can be tolerated by living species ranges from 0.1 MPa (~1 atm) as an atmospheric pressure to 110 MPa (~1100 atm) at the deepest point of Mariana Trench at a depth of 11 km in the western Pacific Ocean [143].

According to the principle of Le Chatelier, if an equilibrated system is exposed to an alteration, the equilibrium is adjusted to object to the alteration [144]. For example, a pressure increase leads to a change in the equilibrium of the system toward its smallest volume during a constant temperature process [145,146]. In addition, the compressibility of biological materials, made of mostly water, is very low. For instance, the compressibility of erythrocytes is about 4×10^{-10} Pa^{-1} [147]. Therefore, by increasing the pressure to a cryobiologically relevant amount, say to 100 MPa, the cellular volume change would be approximately 4%.

The use of pressure as an additional control variable for vitrification is not without its own hazards. In the literature, the effects of high hydrostatic pressure on biological samples are divided into two categories: "physiological high hydrostatic pressure" (pHHP), which is between 1 and 100 MPa, and "non-physiological high hydrostatic pressure" (HHP), which is above 100 MPa [148,149]. Marsland and Zimmerman investigated the biological effects of physiological high hydrostatic pressure (pHHP). They stated that pHHP dissolved the mitotic spindle apparatus and stopped chromosome movement in the eggs of Arbacia punctulata [150–152]. After removing pressure, these effects disappeared [153,154]. Haskin et al. found pressure influences the cytoskeleton of osteosarcoma cells and their responses, which were similar to those under a heat shock [155,156]. Wilson et al. showed morphology and cytoskeleton changes under pHHP [157,158]. Lammi et al. reported the influences of pHHP on articular tissue and confirmed that these effects were reversible and had no impact on the viability of the cells [149]. In terms of pressure tolerance in organs, dog kidneys tolerated 100 MPa for 20 min [159], while rabbit kidneys under 50 MPa were injured after 20 min [160].

The induction of an external shock, such as heat and pressure, was suggested as a mechanism for initiating stress induction [161]. When cells are subjected to stresses such as temperature increase or decrease, heat shock proteins (HSP) are upregulated to respond to these stresses. HSPs not only act as a protection to inhibit severe injuries to cells but also play a role as signals to induce immune responses. Categorized by molecular weight, there are different HSPs in mammalian cells: HSP20, HSP60, HSP70, HSP90, and HSP100 [162]. In the case of imposing pressure of 30 MPa over chondrocytes, only HSP70 was detected [163–165]. Experiments have shown that short-term pHHP on articular cartilage and chondrocytes did not significantly affect cell viability [161]. However, long-term pHHP had different results. For example, Islam et al. reported apoptosis in chondrocytes exposed to 5 MPa for 4 h [166].

When pressure greater than 100 MPa is applied, changes in protein structure and even protein denaturation [167–172], enzyme alteration and dysfunction [173–176], and changes in phospholipid bilayers from fluid-crystalline to a gel-like form [170,172,177,178] were reported. On the one hand, several investigators found induction of apoptosis in cells exposed to 100 MPa pressure, such as murine erythroleukemia cells [179,180] and human lymphoblasts [179]. On the other hand, other researchers did not find a significant effect of 100 MPa pressure on human cell viability [181–183]. As a result, it is hypothesized that the cell cycle plays a role in pressure-induced apoptosis [179,184].

Moving to higher pressures, Frey et al. [161] found that at 200 MPa, cell death occurred through apoptosis identified by symptoms such as DNA fragmentation and morphological changes and that pressurizing to more than 300 MPa has been shown to result in necrosis because of plasma membrane damage [185–187]. In addition, an increase in cytoplasm viscosity was observed [161]. In fact, the rate of increase and duration of pressure substantially affect cell death. Although a fast non-physiological pressure (HHP) rate (the change

in pressure over time) was associated with significant cell death, a short holding time of HHP had a minor impact on cells [161].

3.3. Cytotoxicity of Cryoprotectants in Vitrification

Cryoprotective agents (CPAs) are defined as chemicals that mitigate or eliminate ice damage and reduce high ionic concentrations during cryopreservation [188]. As evidenced by the phase diagram in Figure 1, it is possible to cool cells and tissues without any ice formation with an unlimited amount and concentration of CPAs. In practice, there are two kinds of CPA. The first is "penetrating" or "permeating" CPAs, which have low molecular mass and can pass through the cell membrane and include (among others): ethylene glycol, propylene glycol, dimethylsulfoxide, glycerol, formamide, and methanol. The second is "non-permeating" CPAs with high molecular mass and cannot pass cell membranes, such as trehalose, sucrose, polyethylene glycol, polyvinyl alcohol, and polyvinyl pyrrolidone [189,190]. In fact, CPAs cause changes in hydrogen bonds between water molecules to inhibit ice formation [191]. While the CPA concentration increases, the translational movement of water and CPA molecules reduces [192–194]. The reduction of the water molecule diffusion coefficient postpones the gathering of water molecules in supercooled or heterogeneous regions to form ice crystal clusters, resulting in delaying ice formation (melting point decreases) and promoting glass formation [190]. The translational, vibrational, and rotational movements of water molecules, restricted in the vitreous state, are reduced in aqueous solutions with CPA [195,196]. As a result, the glass transition temperature increases in solutions containing CPAs.

However, concentration-dependent CPA toxicity has been identified as a limitation in cryopreservation [197]. Especially in vitrification, this issue is the main obstacle to reaching the glassy state without any ice formation [198]. Cells and tissues react differently when exposed to different CPAs [199], and most of these differences are related to the conditions of the experiment, including CPA type and concentration, temperature, and exposure time. In this section, we explore the concepts of toxicity of CPA to reduce the amount of toxicity and achieve acceptable cryopreservation.

CPA toxicity has been frequently reported in the field of cryobiology. One of the toxicities related to CPAs is cell membrane toxicity. At the outer and inner surfaces of cell membrane bilayers, there are hydrophilic polar head groups, while in the middle of the cell membrane, there are hydrophobic fatty acid chains. Some factors can increase the permeability of CPAs, such as lipophilicity. On the other hand, increasing molecular size and hydrogen bond formation can reduce a CPA's permeability [200]. For example, in molecular dynamics (MD) simulations, it was shown that sugar molecules interfaced with the lipid head group, while there was no considerable change in the lipid bilayer of cell membranes [201–203]. In cell membranes, CPA molecules can replace water molecules in their hydrogen bonds with phospholipids. For example, trehalose, sucrose, maltose (up to 2 mol/kg), and glucose (up to 4 mol/kg) have been shown to substitute 20–25% of water-phospholipid hydrogen bonds with CPA–phospholipid hydrogen bonds [203]. In addition to the influence on cell membranes, DMSO has another effect called pore formation, occurring in high concentrations of DMSO [204–208]. In this regard, three ranges of concentration can be described. In the first range, the DMSO solution has a relatively low molar concentration (2.5–7.5 mol %) associated with thinning the lipid bilayer membrane by lateral expansion. There is not any bond between DMSO and lipid head groups. Therefore, DMSO molecules stand close to phosphate groups inside the lipid molecules [207]. In the second range of DMSO molar concentration (10–20 mol %), penetration of DMSO molecules inside the lipid bilayer molecules becomes intensive, and DMSO molecules can make transient water pores through cell membranes. Finally, increasing the DMSO molar concentration to more than 25 mol % results in collapsing of the lipid bilayers [207,208].

Warner et al. [209] investigated the toxicity kinetics of multi-CPA mixtures by a toxicity cost function approach and compared the results with experimental data. Their model

in their cell type showed that ethylene glycol and glycerol are relatively non-toxic CPAs compared to formamide, which is a highly toxic CPA. Moreover, by increasing the type of CPAs in the solution, the total toxicity of the solution reduces. Benson et al. [210] have provided a similar model able to quantify the CPA toxicity and optimize equilibration protocols in tissues. Their model shows that time-optimal protocols can perform faster than the non-optimized standard stepwise method but incur more accumulated toxicity. Benson et al. [211] defined the minimization of the toxicity cost function to optimize protocols for CPA addition and removal, while they believed that CPA does not need to be included in the extracellular solution during CPA removal. In addition, they stated that osmotic and mechanical damage due to volume change is insignificant when cell volume is placed within the cell volume tolerance limit.

To sum up, many factors play a role in the CPA toxicity of biospecimens, requiring specific cryoprotocol to reduce cytotoxicity based on cryopreserved biospecimen, CPA type, and freezing method.

4. Bioengineering Aspects of Vitrification

4.1. Necessity of Ultra-Rapid Cooling

The growth of ice crystals can cause severe damage to cells and tissues. Thus, to address this issue, the use of ultra-rapid cooling is needed when low CPA concentrations are used. Ultra-rapid freezing is a cryopreservation technique much faster than slow freezing and even conventional vitrification methods in cryobiology. Slow freezing methods often require expensive programmable freezers with complicated protocols to cryopreserve each type of cell and tissue. On the other hand, the success of any fast-freezing approach is greatly dependent on the CPA concentration, which is generally associated with toxicity in cells and tissues. In short, vitrification approaches will trade the challenge of managing subzero ice formation and water transport via cooling rates in slow or equilibrium protocols for the challenge of managing CPA toxicity and mechanical stresses at above-zero temperatures in vitrification protocols.

4.2. Methods and Devices of Vitrification

Cooling rates are generally limited by conductive heat transfer in tissues greater than 1 mm thick. A number of methods and devices have been presented to maximize heat transfer, and these methods fall into three categories used for rapid freezing: conventional rapid freezing, ultra-rapid freezing, and high-pressure freezing [28,36].

4.2.1. Conventional Rapid Freezing

In the conventional rapid freezing method, a biological sample is immersed directly in a cryogen, such as liquid nitrogen, with a boiling point of −196 °C. In this method, the heat loss from the sample creates an insulating film of evaporated nitrogen around the sample, called the Leidenfrost effect. Therefore, heat loss and cooling rate are reduced [19]. However, this method has been widely used in research and clinical centers due to its simplicity and low cost.

4.2.2. Ultra-Rapid Freezing

Concerning ultra-rapid freezing technology, there are four methods: plunging, spraying, jetting, and metal block [19].

Plunge Freezing

Plunge freezing commenced in the 1950′s in the application of electron microscopy [212]. Among the method of ultra-rapid freezing, this method is less costly, more straightforward, and most used. Plunging involves placing a biological sample either with or without a container directly in liquid cryogens [71,213–227]; however, compared with the conventional rapid freezing method, there are four effective conditions to improve the cooling rate: High entry velocity of the sample into a cryogen (minimum 1 m/s) [228–231]; High

surface-to-volume ratio of the sample (e.g., a copper mesh or a device such as a cryoloop or cryotop) [120–122,125,216,217,222,232,233]; The lowest possible temperature of cryogen (e.g., nitrogen slush or liquid helium) [232,234–239]; Stirring the cryogen in a container to decrease temperature gradients [235,240].

Due to a number of improvements, this approach has a higher cooling rate than conventional rapid freezing; nonetheless, it faces significant challenges in freezing thick biospecimens, such as 1 mm thick tissue.

Spray Freezing

The spray freezing method is the same as plunging, but a sample is reduced to small droplets in order to increase the surface-to-volume ratio of contact area [28]. In this regard, Akiyama et al. [26] developed an inkjet system to create small droplets containing cells. Droplets were placed on a surface cooled by liquid nitrogen. Cooling droplets with a solid surface could prevent the Leidenfrost effect. The volume of droplets was between 40 and 200 pL (10^{-12} L), they achieved a maximum cooling rate of 2.2×10^6 °C/min, and they confirmed the vitrification of droplets by spectroscopy and a high-speed camera. Although a high cooling rate is achievable with this method for CPA-free cryopreservation, this system is limited in scope to cells in suspension, and as such cannot be used for tissue slices or other small tissues.

Jet Freezing

In the jetting method, liquid cryogen is shot toward a sample at a high velocity [241–244]. Katkov et al. [29] designed a device that could shoot a jet of liquid nitrogen to a solid surface containing a sample. The whole cooling process was performed in milliseconds or even microseconds, and they could not measure the sample temperature directly because of the thermal inertia of the thermocouple. Thus, they used glycerol solution with a known critical cooling rate as a function of the concentration and identified vitrification of the medium visually when the medium was completely transparent. They claimed a cooling rate of 10^5 °C/min for a plastic cryovial containing 4 mL 15% glycerol. However, this cooling rate was not measured directly and, as such, may be an overestimation of the cooling rate. This approach may have other problems, such as not eliminating the Leidenfrost effect, completely.

Metal Block Freezing

In metal block freezing, a sample is placed into direct contact with a highly heat-conductive metal block cooled to as low a temperature as possible [232,245–247]. Cold metal block cooling was tried by Simpson in 1941 [248]. After that, several researchers, principally in the field of cryo-electron microscopy, improved this technique (Van Harreveld and Crowell [249], Van Harreveld et al. [250], Heuser et al. [246,247], Boyne [245], Escaig [232], Philips and Boyne [251], Heath [252]). In all these devices, a metal block made of copper or silver is cooled by liquid nitrogen or helium and maintained in an insulating container. By passing cooled nitrogen or helium gas over the surface of the metal block, heat transfer limiting frost formation can be prevented. A sample is placed in a carrier mounted in a holder assembly. Then, this holder falls onto the metal block through guidance, and the rebound of the sample after striking the block is prevented by a spring. This technique was used first for freezing tissues for cryo-electron microscopy, and the results were acceptable (Heuser et al. [246], Hirokawa and Kirino [253], Ichikawa et al. [254], Ornberg and Reese [255], Hirokawa and Heuser [256], Terracio et al. [257], Hirokawa [258], Schnapp and Reese [259], McGuire and Twietmeyer [260], Philips and Boyne [251], Menco [261]). This approach was also developed to freeze cellular suspensions (Chandler and Heuser [262,263], Ornberg and Reese [264], Chandler [265], Wagner and Andrews [266]). This method has an estimated cooling rate of 10^6 °C/min, but only for the surface (Plattner and Bachmann [267]). However, due to cooling just from one side, the depth of vitrification is limited and may not be sufficient to vitrify the entire sample.

Moreover, this technique can damage the biological sample because of the impact onto the cooled surface. In addition, these biological samples were bare without any closed container, which becomes a challenge in clinical applications.

There have been many designs, modifications, developments, and alterations based on the idea of a cold metal block [268–272]. However, reports of these approaches beyond cryo-electron microscopy and into labs or clinical centers have been rare, even though these relatively inexpensive approaches yield good results. This may be due to the complicated designs that make results difficult to reproduce.

4.2.3. High-Pressure Freezing

In high-pressure freezing technology, in one method, a sample is preserved by high-pressure jetting liquid nitrogen [29,60,273–277]. The main issue regarding this method is the Leidenfrost effect due to direct contact between liquid nitrogen and biological sample and damage of the sample because of the direct liquid nitrogen jet. In another method, isochoric (constant volume) can cause high pressure inside the sample due to the increasing ice volume during freezing [278–280]. However, this method of high-pressure freezing cannot be categorized as a vitrification method because of the low cooling rate used in this process [32].

A summary of the freezing techniques, samples tested, corresponding advantages, disadvantages, and achievements is given in Table 2.

Table 2. Different freezing techniques to enhance the cooling rate, suppress ice crystal formation, and reach vitrified biosolution for various applications, including cryomicroscopy and cryopreservation.

Technique	Advantages	Disadvantages	Sample	Result	Ref.
Conventional rapid freezing	-Simple -Less costly -Most widely used	-Low cooling rate -Leidenfrost effect -High CPA concentration	Bovine endothelial cells TE-85 strain human osteosarcoma cells Human breast carcinoma cells	Freeze-fracturing of cells in monolayers or multilayer tissue cultures	[281]
			Human spermatozoa	No difference in motility was detected compared with slow freezing	[282]
			Human spermatozoa	No difference in DNA fragmentation was detected compared with slow freezing	[283]
			Rat ovarian tissue	Follicular pool reduced.	[284]
			Mouse follicle	No significant differences in meiotic spindle formation	[285]
			Human ovarian tissue	Similarity of genes expression in vitrified and non-vitrified groups	[286]
Plunge freezing	-Relative simplicity, low cost, most widely used	-Sophisticated compared to the conventional technique	Human erythrocytes	Two opposing 25–30 μm surface zones were frozen in the apparent absence of ice	[228]
	-Higher cooling rate compared to the conventional method	-Low cooling rate for thick biospecimen	Rat liver tissue	Increasing the cooling rate	[232]
			Maize root epidermal cells	Achieving ice crystals being acceptably small and non-disruptive	[287]
			PtK2 cells	Reducing shrinkage and alteration of the trabecular structure	[217]
			Fibroblasts or epithelial cells derived from Xenopus laevis embryos	Observation of the cytoplasm included interconnected filaments. The general organization was similar to intact cells.	[288]
			Hyphal tip cells of Fusarium acuminatum	Observing all cellular membranes and most organelles due to the transparency of freezing	[222]
			Whole eyes of adult albino mice	The low depth freezing due to the thickness of samples	[289]

Table 2. *Cont.*

Technique	Advantages	Disadvantages	Sample	Result	Ref.
			Slices of rat kidney	Reaching high-quality morphological preservation	[235]
			Antennae of the silk moth, Bombyx mori	Observation of freezing damage just in deeper tissue regions under CPA-free and probably due to natural CPA	[215]
			Bovine oocytes and blastocysts	8% blastocyst yield	[290]
			Murine and bovine oocytes and embryos	73% cleavage rate 7% blastocyst rate	[291]
			Cattle oocytes	55.81% cleavage rate 11.24% blastocyst rate	[292]
Spray freezing	-High cooling rate due to the high surface-to-volume ratio of biospecimen	-Limited to particulates up to 1 µm in diameter -Costly and tedious -Biospecimen damage due to shearing forces in the spray nozzle	5% glycerol-water solution (cryomedia sample without biospecimen)	Preventing large ice compartment A smooth surface of frozen water	[293]
			Paramecium tetraurelia 7S (wild type) cells	No Ca^{+2} influx, which is necessary for induction of membrane fusion.	[294]
			Rat hepatocytes	Higher viability and better morphology in the bulk droplet (3–5 mm diameter) compared to controlled rate freezing	[295]
			3T3 mouse fibroblast cells, human neuroprogenitor cells (NPCs)	90% Viability with CPA concentration less than 0.8 M in 114 nL droplet	[296]
Jet freezing	-Quite high cooling rate due to the high velocity of the cryogen jet -Fast process	-Difficulty in sample handling -Biospecimen damage due to direct jetting with high velocity	Bovine chromaffin cell	Increasing rapid cooling rate up to 40,000 °C/s	[297]
	-High depth of cooling due to cooling from both sides of the specimen at atmospheric pressure	-Non-uniform freezing through the biospecimen -Biospecimen adhesion to cryodevice holder after freezing	Yeast cells	Enhancing the cooling rate to 18,000 °C/s	[243]

Table 2. *Cont.*

Technique	Advantages	Disadvantages	Sample	Result	Ref.
	-Moderate cost of equipment and operation	-Less advantage in tissue samples compared to the cold metal technique	Spinal cord explants from mouse embryos	Retaining the shape of the tissue surface	[242]
			Rat Sertoli cells Human monocytes	High cooling rate even in the absence of any CPA	[298]
			Human embryonic stem cells, human spermatozoa	Higher cell membrane integrity compared to conventional freezing	[299]
			15% glycerol-water solution (cryosolution sample without biospecimen)	Vitrification of 4000 µL of cryosolution	[29,300]
Metal block freezing	-High thermal diffusivity of copper and silver block	-The high cost and challenging nature of manufacturing and operating copper and silver blocks due to their softness -Biospecimen damage due to crushing, shearing, and bounce -Low depth of cooling due to cooling from just one side -Bare biospecimen without container causing contamination	Red blood cells	Modifying ice microcrystals appeared at a depth of 25–30 µm, while it was already observed at a depth of 12–15 µm.	[232]
			Mouse liver tissue	Obtaining acceptable blocks of preserved tissues for cryofixation	[249]
			Mouse liver and diaphragm tissues, Isolated strands of celery phloem, rose phloem, pea root tip, and Chinese cabbage and tobacco leaf tissue	Using the heat-conductive properties of copper to increase the cooling rate The tissue surface layer was ice-free up to 12 µm in depth.	[269]
			Goat testicular cell	74.8% cell viability	[301]
			Leydig cells (murine cell line TM3)	Superior cell growth, mitochondrial activity, and cytoplasmic esterase enzyme activity than the conventional method	[302]
			Mouse myoblast C2C12 cells, rat primary mesenchymal stem cells	More than 80% cell viability in 40 pL CPA-free droplet	[26]
			Cat ovarian tissue	Normal follicles after thawing	[303]
			Cow blastocyst	69% hatching rate	[304]

Table 2. *Cont.*

Technique	Advantages	Disadvantages	Sample	Result	Ref.
High Pressure (hyperbaric) freezing	-Higher depth of cooling due to cooling from both sides of the specimen under high pressure -Lower CPA concentration -Ability to cool ultra-rapidly thick biospecimen such as tissue	-Biospecimen preservation quality for cryomicroscopy is not as good as well-prepared biospecimen under ultra-rapidly frozen at atmospheric pressure.	Rat brain tissue	Preventing large ice crystal formation in tissue up to 0.5 mm thick	[274]
	-Lower rate of ice crystal formation and growth	-The least known and least tested technique -High temperature and low cooling rate for the isochoric condition	Beef liver catalase crystals	Increasing the depth of vitrification approximately ten times larger with freezing at high pressure (2 Kbar)	[60]
			Ascites tumor cell	Obtaining the same quality of vitrification without CPA	[273]
			Rat cartilage tissue	Enhancing the quality of preserved chondrocytes than those preserved by chemical fixation	[275]
			Bovine and rat parathyroid cell	Excellent preservation of ultrastructure of cells	[276]
			Actomyosin system of Physarum polycephalum	Avoiding artificial alterations observed in chemical fixation	[277]
			Rat heart	The first freezing of mammalian organs without CPA at −4 °C, 41 MPa, and under the isochoric condition	[278]
			Fish muscle tissue	No cellular dehydration and maintaining the morphology of the frozen tissue under the isochoric condition	[279]
			Madin-Darby canine Kidney epithelial cells (MDCK)	60% and 18% cell viability during 60 and 120 min at –10 °C under the isochoric condition	[280]
			Human red blood cells	8% or less hemolysis of RBCs with 5% DMSO (*v*/*v*) or 8% glycerol (*v*/*v*) and 120 MPa pressure	[58]

5. Summary

This review investigates the physiochemical concepts involved in cryobiology, various cryopreserved biospecimens, and devices designed to improve biospecimens' viability after thawing. Up to now, a few manuscripts have had an interdisciplinary viewpoint of all factors playing a role in cryopreservation. Here we study several significant parameters influencing the vitrification technology from different aspects.

Recently, vitrification has been considered widely in stem cells, cell therapy, reproductive technology, and transplantation. Many protocols, methods, devices, and technologies have been used and tested to improve vitrification. However, there are impediments to vitrification technology, which can be solved by considering all disciplines involved in cryopreservation, such as physical chemistry, biomathematics, engineering, and biology.

CPA toxicity is a significant concern that should be tackled through an interdisciplinary approach, including physical chemistry techniques such as differential scanning calorimetry (DSC) and mechanical and mathematical modeling of transport and toxicity [208,210]. It is essential to define low-CPA concentration cryoprotocols or even CPA-free methods to reduce cytotoxicity and cell mechanical damage.

The idea of "non-harmful" ice crystals in cryobiology can enhance cell and tissue cryopreservation [27]. This idea requires ultra-rapid cooling with techniques that can increase heat transfer. High heat transfer in the ultra-rapid method is limited not only by the thermal properties of devices but also by the biospecimen thickness and cryosolution volume, imposing substantial restrictions against this technique. In this regard, many devices and methods have been introduced and developed to address this matter.

The warming process is another concern in cryobiology. Cryosolutions with high CPA concentrations, due to the high amount of vitrification in the solution during cooling, ice recrystallization is a significant obstacle to cell and tissue viability in the warming process. Under these circumstances, a high warming rate is required to suppress devitrification and large ice crystal formation [305]. In fact, there are a number of engineering approaches to increase warming rates in ever larger tissues, including laser, microwave, and induction-based warming [306–309]. However, in cryosolutions with low CPA concentrations under ultra-rapid cooling, it is plausible that ice recrystallization could be eliminated at a lower warming rate when only tiny ice crystals form in the cooling process [69].

To sum up, there are several limitations for the vitrification method in practical applications, such as low biospecimen volume, contamination, small tissue thickness, complicated techniques, and devices that need to be addressed through interdisciplinary investigations. There is no doubt that cryopreserved specimens will be highly demanded in the future, particularly in cancer cell therapy for cancer and on-shelf organ cryopreservation for transplantation [310].

6. Conclusions

In this review, we presented some basic and interdisciplinary notions applicable to cryopreservation and a diverse cryopreserved biospecimen with different methods and devices, showing various results due to the type of cells and tissues with different cooling rates and cryoprotocols. Hence, it is essential to pay more attention to fundamental interdisciplinary concepts of cryobiology to build a bridge between all current gaps in the literature and achieve sustainability in this realm of technology.

Author Contributions: Conceptualization: M.A. and J.D.B.; investigation: M.A.; resources: J.D.B.; writing—original draft preparation: M.A.; writing—review and editing: M.A. and J.D.B.; supervision: J.D.B.; funding acquisition: J.D.B. All authors have read and agreed to the published version of the manuscript.

Funding: This research was funded by the National Science and Engineering Research Council (NSERC RGPIN-2017-06346 to JB).

Conflicts of Interest: The authors declare no conflict of interest.

References

1. Muraca, M.; Gerunda, G.; Neri, D.; Vilei, M.T.; Granato, A.; Feltracco, P.; Meroni, M.; Giron, G.; Burlina, A.B. Hepatocyte Transplantation as a Treatment for Glycogen Storage Disease Type 1a. *Lancet* **2002**, *359*, 317–318. [CrossRef] [PubMed]
2. Najimi, M.; Sokal, E. Update on Liver Cell Transplantation. *J. Pediatric Gastroenterol. Nutr.* **2004**, *39*, 311–319. [CrossRef] [PubMed]
3. Sokal, E.M.; Smets, F.; Bourgois, A.; Maldergem, V.; Buts, J.-P.; Reding, R.; Bernard Otte, J.; Evrard, V.; Latinne, D.; Vincent, M.F. Transplantation in a 4-Year-Old Girl with Peroxisomal Biogenesis Disease: Technique, Safety, and Metabolic Follow-Up1. *Transplantation* **2003**, *76*, 735–738. [CrossRef] [PubMed]
4. Strom, S.C.; Fisher, R.A.; Thompson, M.T.; Sanyal, A.J.; Cole, P.E.; Ham, J.M.; Posner, M.P. Hepatocyte Transplantation as a Bridge to Orthotopic Liver Transplantation in Terminal Liver Failure. *Transplantation* **1997**, *63*, 559–569. [CrossRef] [PubMed]
5. Stéphenne, X.; Najimi, M.; Sokal, E.M. Hepatocyte Cryopreservation: Is It Time to Change the Strategy? *World J. Gastroenterol.* **2010**, *16*, 1–14. [CrossRef] [PubMed]
6. Tas, R.P.; Sampaio-Pinto, V.; Wennekes, T.; van Laake, L.W.; Voets, I.K. From the Freezer to the Clinic. *Embo Rep.* **2021**, *22*, e52162. [CrossRef]
7. Shi, Q.; Xie, Y.; Wang, Y.; Li, S. Vitrification versus Slow Freezing for Human Ovarian Tissue Cryopreservation: A Systematic Review and Meta-Anlaysis. *Sci. Rep.* **2017**, *7*, 8538. [CrossRef]
8. Tokuda, K.; Ikemoto, T.; Saito, Y.; Miyazaki, K.; Yamashita, S.; Yamada, S.; Imura, S.; Morine, Y.; Shimada, M. The Fragility of Cryopreserved Insulin-Producing Cells Differentiated from Adipose-Tissue-Derived Stem Cells. *Cell Transpl.* **2020**, *29*. [CrossRef]
9. O'Brien, E.; Esteso, M.C.; Castaño, C.; Toledano-Díaz, A.; Bóveda, P.; Martínez-Fresneda, L.; López-Sebastián, A.; Martínez-Nevado, E.; Guerra, R.; López Fernández, M. Effectiveness of Ultra-Rapid Cryopreservation of Sperm from Endangered Species, Examined by Morphometric Means. *Theriogenology* **2019**, *129*, 160–167. [CrossRef]
10. Kaczmarczyk, A.; Funnekotter, B.; Turner, S.R.; Bunn, E.; Bryant, G.; Hunt, T.E.; Mancera, R.L. Development of Cryopreservation for Loxocarya Cinerea-an Endemic Australian Plant Species Important for Post-Mining Restoration. *Cryo Lett.* **2013**, *34*, 508–519.
11. Edesi, J.; Tolonen, J.; Ruotsalainen, A.L.; Aspi, J.; Häggman, H. Cryopreservation Enables Long-Term Conservation of Critically Endangered Species Rubus Humulifolius. *Biodivers. Conserv.* **2020**, *29*, 303–314. [CrossRef]
12. Decelle, J.; Veronesi, G.; Gallet, B.; Stryhanyuk, H.; Benettoni, P.; Schmidt, M.; Tucoulou, R.; Passarelli, M.; Bohic, S.; Clode, P.; et al. Subcellular Chemical Imaging: New Avenues in Cell Biology. *Trends Cell Biol.* **2020**, *30*, 173–188. [CrossRef] [PubMed]
13. Penninckx, F.; Poelmans, S.; Kerremans, R.; De Loecker, W. Erythrocyte Swelling after Rapid Dilution of Cryoprotectants and Its Prevention. *Cryobiology* **1984**, *21*, 25–32. [CrossRef] [PubMed]
14. Karlsson, J.O.M.; Cravalho, E.G.; Toner, M. A Model of Diffusion-limited Ice Growth inside Biological Cells during Freezing. *J. Appl. Phys.* **1998**, *75*, 4442. [CrossRef]
15. Pan, J.; Shu, Z.; Zhao, G.; Ding, W.; Ren, S.; Sekar, P.K.; Peng, J.; Chen, M.; Gao, D. Towards Uniform and Fast Rewarming for Cryopreservation with Electromagnetic Resonance Cavity: Numerical Simulation and Experimental Investigation. *Appl. Therm. Eng.* **2018**, *140*, 787–798. [CrossRef]
16. Benson, J. Ultra-Rapid Tissue Cryopreservation Method and Apparatus. U.S. Patent 9,936,690 B2, 20 November 2018.
17. Wolfe, J.; Bryant, G. Cellular Cryobiology: Thermodynamic Amd Mechanical Effects. *Int. J. Refrig.* **2001**, *24*, 438–450. [CrossRef]
18. Gao, D.; Liu, J.; Liu, C.; McGann, L.; Watson, P.; Kleinhans, F.; Mazur, P.; Critser, E.; Critser, J. Andrology: Prevention of Osmotic Injury to Human Spermatozoa during Addition and Removal of Glycerol. *Hum. Reprod.* **1995**, *10*, 1109–1122. [CrossRef]
19. Sherman, J.K. Synopsis of the Use of Frozen Human Semen since 1964: State of the Art of Human Semen Banking. *Fertil. Steril.* **1973**, *24*, 397–412. [CrossRef]
20. Schneider, U.; Mazur, P. Osmotic Consequences of Cryoprotectant Permeability and Its Relation to the Survival of Frozen-Thawed Embryos. *Theriogenology* **1984**, *21*, 68–79. [CrossRef]
21. Mazur, P.; Schneider, U. Osmotic Responses of Preimplantation Mouse and Bovine Embryos and Their Cryobiological Implications. *Cell Biophys.* **1986**, *8*, 259–285. [CrossRef]
22. Leibo, S.P. Cryobiology: Preservation of Mammalian Embryos. In *Genetic Engineering of Animals*; Springer: Boston, MA, USA, 1986; pp. 251–272. [CrossRef]
23. Critser, J.; Huse-Benda, A.; Aaker, D.; Arneson, B.; Ball, D. Cryopreservation of Human Spermatozoa. III. The Effect of Cryoprotectants on Motility. *Fertil. Steril.* **1988**, *50*, 314–320. [CrossRef] [PubMed]
24. Wowk, B. Thermodynamic Aspects of Vitrification. *Cryobiology* **2010**, *60*, 11–22. [CrossRef] [PubMed]
25. Uhlmann, D.R. A Kinetic Treatment of Glass Formation. *J. Non-Cryst. Solids* **1972**, *7*, 337–348. [CrossRef]
26. Akiyama, Y.; Shinose, M.; Watanabe, H. Cryoprotectant-Free Cryopreservation of Mammalian Cells by Superflash Freezing. *Proc. Natl. Acad. Sci. USA* **2019**, *116*, 7738–7743. [CrossRef] [PubMed]
27. Huebinger, J.; Han, H.M.; Hofnagel, O.; Vetter, I.R.; Bastiaens, P.I.H.; Grabenbauer, M. Direct Measurement of Water States in Cryopreserved Cells Reveals Tolerance toward Ice Crystallization. *Biophys. J.* **2016**, *110*, 840–849. [CrossRef]
28. Gilkey, J.C.; Staehelin, L.A. Advances in Ultrarapid Freezing for the Preservation of Cellular Ultrastructure. *J. Electron Microsc. Tech.* **1986**, *3*, 177–210. [CrossRef]
29. Katkov, I.I.; Bolyukh, V.F.; Sukhikh, G.T. KrioBlast TM as a New Technology of Hyper-Fast Cryopreservation of Cells and Tissues. Part, I. Thermodynamic Aspects and Potential Applications in Reproductive and Regenerative Medicine. *Bull. Exp. Biol. Med.* **2018**, *164*, 530–535. [CrossRef]

30. Miyata, K.; Hayakawa, S.; Kajiwara, K.; Kanno, H. Supercooling and Vitrification of Aqueous Glycerol Solutions at Normal and High Pressures. *Cryobiology* **2012**, *65*, 113–116. [CrossRef]
31. Richter, K. High-Density Morphologies of Ice in High-Pressure Frozen Biological Specimens. *Ultramicroscopy* **1994**, *53*, 237–249. [CrossRef]
32. Preciado, J.; Rubinsky, B. Isochoric Preservation: A Novel Characterization Method. *Cryobiology* **2010**, *60*, 23–29. [CrossRef]
33. Ukpai, G.; Năstase, G.; Şerban, A.; Rubinsky, B. Pressure in Isochoric Systems Containing Aqueous Solutions at Subzero Centigrade Temperatures. *PLoS ONE* **2017**, *12*, e0183353. [CrossRef] [PubMed]
34. Brüggeller, P.; Mayer, E. Complete Vitrification in Pure Liquid Water and Dilute Aqueous Solutions. *nature* **1980**, *288*, 569–571. [CrossRef]
35. Grout, B.W.W.; Morris, G.J. Contaminated Liquid Nitrogen Vapour as a Risk Factor in Pathogen Transfer. *Theriogenology* **2009**, *71*, 1079–1082. [CrossRef]
36. Severs, N.J.; Newman, T.M.; Shotton, D.M. A Practical Introduction to Rapid Freezing Techniques. In *Rapid Freezing, Freeze Fracture and Deep Etching*; Severs, N., Shotton, D., Eds.; Wiley-Liss: New York, NY, USA, 1995; pp. 31–49.
37. Ickes, L.; Welti, A.; Hoose, C.; Chemical, U.L. Classical Nucleation Theory of Homogeneous Freezing of Water: Thermodynamic and Kinetic Parameters. *Phys. Chem. Chem. Phys.* **2015**, *17*, 5514–5537. [CrossRef] [PubMed]
38. Gibbs, A.; Willard, J. On the Equilibrium of Heterogeneous Substances. *Trans. Conn. Acad. Arts Sci.* **1879**, *3*, 108–248.
39. Koop, T.; Murray, B.J. A Physically Constrained Classical Description of the Homogeneous Nucleation of Ice in Water. *J. Chem. Phys.* **2016**, *145*, 211915. [CrossRef]
40. Kauzmann, W. The Nature of the Glassy State and the Behavior of Liquids at Low Temperatures. *Chem. Rev.* **1948**, *43*, 219–256. [CrossRef]
41. Jung, S.; Tiwari, M.; Doan, N.; Poulikakos, D. Mechanism of Supercooled Droplet Freezing on Surfaces. *Nat. Commun.* **2012**, *3*, 615. [CrossRef]
42. MacKenzie, A.P. Non-Equilibrium Freezing Behaviour of Aqueous Systems. *Philos. Trans. R. Soc. London. B Biol. Sci.* **1977**, *278*, 167–189. [CrossRef]
43. Rasmussen, D.H. Ice Formation in Aqueous Systems. *J. Microsc.* **1982**, *128*, 167–174. [CrossRef]
44. Clark, G.L. *Applied X-rays*, 3rd ed.; The McGraw-Hill Book Company, Inc.: New York, NY, USA, 1940.
45. Randall, J.T. *Diffraction of X-rays and Electrons by Amorphous Solids, Liquids and Gases*; John Wiley and Sons, Inc.: New York, NY, USA, 1934.
46. Boutron, P.; Kaufmann, A. Stability of the Amorphous State in the System Water-Glycerol-Dimethylsulfoxide. *Cryobiology* **1978**, *15*, 93–108. [CrossRef] [PubMed]
47. Boutron, P.; Kaufmann, A. Stability of the Amorphous State in the System Water—1,2-Propanediol. *Cryobiology* **1979**, *16*, 557–568. [CrossRef] [PubMed]
48. Boutron, P.; Kaufmann, A. Stability of the Amorphous State in the System Water-Glycerol-Ethylene Glycol. *Cryobiology* **1979**, *16*, 83–89. [CrossRef] [PubMed]
49. Boutron, P.; Kaufmann, A.; Van Dang, N. Maximum in the Stability of the Amorphous State in the System Water-Glycerol-Ethanol. *Cryobiology* **1979**, *16*, 372–389. [CrossRef]
50. Baudot, A.; Alger, L.; Boutron, P. Glass-Forming Tendency in the System Water-Dimethyl Sulfoxide. *Cryobiology* **2000**, *40*, 151–158. [CrossRef]
51. Baudot, A.; Cacela, C.; Duarte, M.; Cryobiology, R.F. Thermal Study of Simple Amino-Alcohol Solutions. *Cryobiology* **2002**, *44*, 150–160. [CrossRef]
52. Baudot, A.; Cryobiology, V.O. Thermal Properties of Ethylene Glycol Aqueous Solutions. *Cryobiology* **2004**, *48*, 283–294. [CrossRef]
53. Wowk, B.; Darwin, M.; Harris, S.B.; Russell, S.R.; Rasch, C.M. Effects of Solute Methoxylation on Glass-Forming Ability and Stability of Vitrification Solutions. *Cryobiology* **1999**, *39*, 215–227. [CrossRef]
54. Persidsky, M.D. Cryopreservation under High Hydrostatic Pressure. *Cryobiology* **1971**, *8*, 380. [CrossRef]
55. Dahl, R.; Staehelin, L.A. Highpressure Freezing for the Preservation of Biological Structure: Theory and Practice. *J. Electron Microsc. Tech.* **1989**, *13*, 165–174. [CrossRef]
56. Erk, I.; Nicolas, G.; Caroff, A.; Lepault, J. Electron Microscopy of Frozen Biological Objects: A Study Using Cryosectioning and Cryosubstitution. *J. Microsc.* **1998**, *189*, 236–248. [CrossRef] [PubMed]
57. Ugraitskaya, S.V.; Shishova, N.V.; Valeeva, E.R.; Kaurova, S.A.; Shvirst, N.E.; Fesenko, E.E. Cryopreservation of HeLa Cells at a High Hydrostatic Pressure of 1.0–1.5 Kbar. *Biophys. (Russ. Fed.)* **2021**, *66*, 98–106. [CrossRef]
58. Greer, N. Freezing under Pressure: A New Method for Cryopreservation. *Cryobiology* **2015**, *70*, 66–70. [CrossRef] [PubMed]
59. Mickelson, D.M.; Attig, J.W. *Glacial Processes Past and Present*, 1st ed.; Special Paper: Madison, WI, USA, 1999.
60. Sartori, N.; Richter, K.; Dubochet, J. Vitrification Depth Can Be Increased More than 10-fold by High-pressure Freezing. *J. Microsc.* **1993**, *172*, 55–61. [CrossRef]
61. Wowk, B.; Fahy, G. 21. Ice Nucleation and Growth in Concentrated Vitrification Solutions. *Cryobiology* **2007**, *55*, 330. [CrossRef]
62. Hey, J.M.; Macfarlane, D.R. Crystallization of Ice in Aqueous Solutions of Glycerol and Dimethyl Sulfoxide: 1. A Comparison of Mechanisms. *Cryobiology* **1996**, *33*, 205–216. [CrossRef] [PubMed]
63. MacKenzie, A.P. Death of Yeast in the Course of Slow Warming. In *The Frozen Cell*; Wolstenholme, C.A., O'Connor, M., Eds.; Churchill: London, UK, 1970; pp. 89–96.

64. Mazur, P. The Role of Intracellular Freezing in the Death of Cells Cooled at Supraoptimal Rates. *Cryobiology* **1977**, *14*, 251–272. [CrossRef]
65. Zieger, M.A.J.; Tredget, E.E.; McGann, L.E. Mechanisms of Cryoinjury and Cryoprotection in Split-Thickness Skin. *Cryobiology* **1996**, *33*, 376–389. [CrossRef]
66. Acker, J. Cell–Cell Contact Affects Membrane Integrity after Intracellular Freezing. *Cryobiology* **2000**, *40*, 54–63. [CrossRef]
67. Mazur, P.; Leibo, S. A Two-Factor Hypothesis of Freezing Injury: Evidence from Chinese Hamster Tissue-Culture Cells. *Exp. Cell Res.* **1972**, *71*, 345–355. [CrossRef]
68. De Graaf, I.A.M.; Koster, H.J. Cryopreservation of Precision-Cut Tissue Slices for Application in Drug Metabolism Research. *Toxicol. Vitr.* **2003**, *17*, 1–17. [CrossRef] [PubMed]
69. Amini, M.; Benson, J.D. Investigation of Cryoprotectant Thermophysical Properties in the Fast Cooling Cryopreservation by DSC Technique. *Cryobiology* **2022**, *109*, 34. [CrossRef]
70. Angell, C.A. Supercooled Water. In *Water-A Comprehensive Treatise*; Franks, F., Ed.; Plenum Press: New York, NY, USA, 1982; pp. 1–81.
71. Bank, H. Visualization of Freezing Damage. II. Structural Alterations during Warming. *Cryobiology* **1973**, *10*, 157–170. [CrossRef]
72. Rall, W.F.; Reid, D.S.; Polge, C. Analysis of Slow-Warming Injury of Mouse Embryos by Cryomicroscopical and Physiochemical Methods. *Cryobiology* **1984**, *21*, 106–121. [CrossRef] [PubMed]
73. Nei, T. Growth of Ice Crystals in Frozen Specimens. *J. Microsc.* **1973**, *99*, 227–233. [CrossRef]
74. Mazur, P. Freezing of Living Cells: Mechanisms and Implications. *Am. J. Physiol.-Cell Physiol.* **1984**, *247*, C125–C142. [CrossRef]
75. Li, A.P.; Gorycki, P.D.; Hengstler, J.G.; Kedderis, G.L.; Koebe, H.G.; Rahmani, R.; De Sousas, G.; Silva, J.M.; Skett, P. Present Status of the Application of Cryopreserved Hepatocytes in the Evaluation of Xenobiotics: Consensus of an International Expert Panel. *Chem.-Biol. Interact.* **1999**, *121*, 117–123. [CrossRef]
76. Rijntjes, P.J.M.; Moshage, H.J.; Van Gemert, P.J.L.; De Waal, R.; Yap, S.H. Cryopreservation of Adult Human Hepatocytes. *J. Hepatol.* **1986**, *3*, 7–18. [CrossRef]
77. De Sousa, G.; Langouët, S.; Nicolas, F.; Lorenzon, G.; Placidi, M.; Rahmani, R.; Guillouzo, A. Increase of Cytochrome P-450 1A and Glutathione Transferase Transcripts in Cultured Hepatocytes from Dogs, Monkeys, and Humans after Cryopreservation. *Cell Biol. Toxicol.* **1996**, *12*, 351–358. [CrossRef]
78. Ostrowska, A.; Bode, C.D.; Pruss, J.; Bilir, B.; Smith, G.D.; Zeisloft, S. Investigation of Functional and Morphological Integrity of Freshly Isolated and Cryopreserved Human Hepatocytes. *Cell Tissue Bank.* **2000**, *1*, 55–68. [CrossRef]
79. Luyet, B. *The Vitrification of Organic Colloids and of Protoplasme*; Biodynamica: Whitefish, MT, USA, 1937.
80. Bunge, R.G.; Sherman, J.K. Fertilizing Capacity of Frozen Human Spermatozoa. *Nature* **1953**, *172*, 767–768. [CrossRef] [PubMed]
81. Wishnies, S.M.; Parrish, A.R.; Sipes, I.G.; Gandolfi, A.J.; Putnam, C.W.; Krumdieck, C.L.; Brendel, K. Biotransformation Activity in Vitrified Human Liver Slices. *Cryobiology* **1991**, *28*, 216–226. [CrossRef] [PubMed]
82. De Kanter, R.; Koster, H.J. Cryopreservation of Rat and Monkey Liver Slices. *Altern. Lab. Anim.* **1995**, *23*, 653–665. [CrossRef]
83. De Kanter, R.; Olinga, P.; De Jager, M.H.; Merema, M.T.; Meijer, D.K.F.; Groothius, G.M.M. Organ Slices as an in Vitro Test System for Drug Metabolism in Human Liver, Lung and Kidney. *Toxicol. Vitr.* **1999**, *13*, 737–744. [CrossRef] [PubMed]
84. de Graaf, I.A.M.; van der Voort, D.; Brits, J.H.F.G.; Koster, H.J. Increased Post-Thaw Viability and Phase I and II Biotransformation Activity in Cryopreserved Rat Liver Slices after Improvement of a Fast-Freezing Method. *Drug Metab. Dispos.* **2000**, *28*, 1100–1106.
85. Day, S.H.; Nicoll-Griffith, D.A.; Silva, J.M. Cryopreservation of Rat and Human Liver Slices by Rapid Freezing. *Cryobiology* **1999**, *38*, 154–159. [CrossRef]
86. Powis, G.; Santone, K.S.; Melder, D.C.; Thomas, L.; Moore, D.J.; Wilke, T.J. Cryopreservation of Rat and Dog Hepatocytes for Studies of Xenobiotic Metabolism and Activation. *Drug Metab. Dispos.* **1987**, *15*, 826–832.
87. Coundouris, J.A.; Grant, M.H.; Simpson, J.G.; Hawksworth, G.M. Drug Metabolism and Viability Studies in Cryopreserved Rat Hepatocytes. *Cryobiology* **1990**, *27*, 288–300. [CrossRef]
88. Diener, B.; Utesch, D.; Beer, N.; Dürk, H.; Oesch, F. A Method for the Cryopreservation of Liver Parenchymal Cells for Studies of Xenobiotics. *Cryobiology* **1993**, *30*, 116–127. [CrossRef]
89. Maas, W.J.M.; De Graaf, I.A.M.; Schoen, E.D.; Koster, H.J.; Van De Sandt, J.J.M.; Groten, J.P. Assessment of Some Critical Factors in the Freezing Technique for the Cryopreservation of Precision-Cut Rat Liver Slices. *Cryobiology* **2000**, *40*, 250–263. [CrossRef]
90. Pegg, D.E. Ice Crystals in Tissues and Organs. In *The Biophysics of Organ Cryopreservation*; Springer: Boston, MA, USA, 1987. [CrossRef]
91. Bischof, J.C.; Ryan, C.M.; Tompkins, R.G.; Yarmush, M.L.; Toner, M. Ice Formation in Isolated Human Hepatocytes and Human Liver Tissue. *Asaio, J.* **1997**, *43*, 271–278. [CrossRef] [PubMed]
92. Rapatz, G.; Luyet, B. Microscopic Observations on the Development of the Ice Phase in the Freezing of Blood. *Biodynamica* **1960**, *8*, 195–239.
93. Takahashi, T.; Hirsh, A. Calorimetric Studies of the State of Water in Deeply Frozen Human Monocytes. *Biophys. J.* **1985**, *47*, 373–380. [CrossRef] [PubMed]
94. Yamane, H.; Ohshima, H.; Kondod, T. Freezing Behaviour of Microencapsulated Water. *J. Microencapsul.* **1992**, *9*, 279–286. [CrossRef]

95. Peyridieu, J.F.; Baudot, A.; Boutron, P.; Mazuer, J.; Odin, J.; Ray, A.; Chapelier, E.; Payen, E.; Descotes, J.L. Critical Cooling and Warming Rates to Avoid Ice Crystallization in Small Pieces of Mammalian Organs Permeated with Cryoprotective Agents. *Cryobiology* **1996**, *33*, 436–446. [CrossRef] [PubMed]
96. Kliesch, S.; Kamischke, A.; Cooper, T.G.; Nieschlag, E. Cryopreservation of Human Spermatozoa. In *Andrology: Male Reproductive Health and Dysfunction*; Springer: Berlin/Heidelberg, Germany, 2010; Volume 12, pp. 505–520. [CrossRef]
97. Endo, Y.; Fujii, Y.; Shintani, K.; Seo, M.; Motoyama, H.; Funahashi, H. Simple Vitrification for Small Numbers of Human Spermatozoa. *Reprod. Biomed. Online* **2012**, *24*, 301–307. [CrossRef]
98. Herrler, A.; Eisner, S.; Bach, V.; Weissenborn, U.; Beier, H.M. Cryopreservation of Spermatozoa in Alginic Acid Capsules. *Fertil. Steril.* **2006**, *85*, 208–213. [CrossRef]
99. Shufaro, Y.; Stein, A.; Shufaro, Y.; Hadar, S.; Fisch, B.; Pinkas, H. Successful Use of the Cryolock Device for Cryopreservation of Scarce Human Ejaculate and Testicular Spermatozoa. *Wiley Online Libr.* **2015**, *3*, 220–224. [CrossRef]
100. Liu, F.; Zou, S.S.; Zhu, Y.; Sun, C.; Liu, Y.F.; Wang, S.S.; Shi, W.B.; Zhu, J.J.; Huang, Y.H.; Li, Z. A Novel Micro-Straw for Cryopreservation of Small Number of Human Spermatozoon. *Asian J. Androl.* **2016**, *19*, 326–329. [CrossRef]
101. Berkovitz, A.; Miller, N.; Silberman, M.; Belenky, M.; Itsykson, P. A Novel Solution for Freezing Small Numbers of Spermatozoa Using a Sperm Vitrification Device. *Hum. Reprod.* **2018**, *33*, 1975–1983. [CrossRef]
102. Paffoni, A.; Palini, S. There Is Another New Method for Cryopreserving Small Numbers of Human Sperm Cells. *Ann. Transl. Med.* **2019**, *7*, S17. [CrossRef] [PubMed]
103. Feng, H.; Xu, Y.; Yang, T. Study on Leidenfrost Effect of Cryoprotectant Droplets on Liquid Nitrogen with IR Imaging Technology and Non-Isothermal Crystallization Kinetics Model. *Int. J. Heat Mass Transf.* **2018**, *127*, 413–421. [CrossRef]
104. XU, Y.; WANG, T.; DENG, X.; YANG, T.; WANG, C.; CAO, J.; FANG, L. Analysis on the Leidenfrost Effect of Cryoprotectant Microdroplets on the Liquid Nitrogen Surface. *Sci. Sin. Technol.* **2017**, *47*, 190–196. [CrossRef]
105. Isachenko, V.; Isachenko, E.; Katkov, I.I.; Montag, M.; Dessole, S.; Nawroth, F.; Van Der Ven, H. Cryoprotectant-Free Cryopreservation of Human Spermatozoa by Vitrification and Freezing in Vapor: Effect on Motility, DNA Integrity, and Fertilization Ability. *Biol. Reprod.* **2004**, *71*, 1167–1173. [CrossRef] [PubMed]
106. Bielanski, A. A Review of the Risk of Contamination of Semen and Embryos during Cryopreservation and Measures to Limit Cross-Contamination during Banking to Prevent Disease Transmission in ET Practices. *Theriogenology* **2012**, *77*, 467–482. [CrossRef]
107. HARRISON, A.P. Survival of Bacteria upon Repeated Freezing and Thawing. *J. Bacteriol.* **1955**, *70*, 711–715. [CrossRef]
108. Piasecka-Serafin, M. The Effect of the Sediment Accumulated in Containers under Experimental Conditions on the Infection of Semen Stored Directly in Liquid Nitrogen (-196 Degree C). *Bull. De L"Acad. Pol. Des Sciences. Ser. Des Sci. Biol.* **1972**, *20*, 263–267.
109. Schafer, T.; Everett, J.; Silver, G.; Came, P.E. Biohazard: Virus-Contaminated Liquid Nitrogen. *Science* **1976**, *191*, 24–26. [CrossRef]
110. Tedder, R.S.; Zuckerman, M.A.; Brink, N.S.; Goldstone, A.H.; Fielding, A.; Blair, S.; Patterson, K.G.; Hawkins, A.E.; Gormon, A.M.; Heptonstall, J. Hepatitis B Transmission from Contaminated Cryopreservation Tank. *Lancet* **1995**, *346*, 137–140. [CrossRef]
111. Cobo, A.; Bellver, J.; De Los Santos, M.J.; Remohí, J. Viral Screening of Spent Culture Media and Liquid Nitrogen Samples of Oocytes and Embryos from Hepatitis B, Hepatitis C, and Human Immunodeficiency Virus Chronically Infected Women Undergoing in Vitro Fertilization Cycles. *Fertil. Steril.* **2012**, *97*, 74–78. [CrossRef]
112. Molina, I.; Mari, M.; Martínez, J.V.; Novella-Maestre, E.; Pellicer, N.; Pemán, J. Bacterial and Fungal Contamination Risks in Human Oocyte and Embryo Cryopreservation: Open versus Closed Vitrification Systems. *Fertil. Steril.* **2016**, *106*, 127–132. [CrossRef] [PubMed]
113. Deen, G.F.; Broutet, N.; Xu, W.; Knust, B.; Sesay, F.R.; McDonald, S.L.R.; Ervin, E.; Marrinan, J.E.; Gaillard, P.; Habib, N. Ebola RNA Persistence in Semen of Ebola Virus Disease Survivors—Final Report. *N. Engl. J. Med.* **2017**, *377*, 1428–1437. [CrossRef] [PubMed]
114. Nicastri, E.; Castilletti, C.; Liuzzi, G.; Iannetta, M.; Capobianchi, M.R.; Ippolito, G. Persistent Detection of Zika Virus RNA in Semen for Six Months after Symptom Onset in a Traveller Returning from Haiti to Italy, February 2016. *Eurosurveillance* **2016**, *21*, 30314. [CrossRef]
115. Bielanski, A. *Biosafety in Embryos and Semen Cryopreservation, Storage, Management and Transport*; Springer: New York, NY, USA, 2014; pp. 429–465. [CrossRef]
116. Bielanski, A.; Nadin-Davis, S.; Sapp, T.; Lutze-Wallace, C. Viral Contamination of Embryos Cryopreserved in Liquid Nitrogen. *Cryobiology* **2000**, *40*, 110–116. [CrossRef] [PubMed]
117. Morris, G.J. The Origin, Ultrastructure, and Microbiology of the Sediment Accumulating in Liquid Nitrogen Storage Vessels. *Cryobiology* **2005**, *50*, 231–238. [CrossRef] [PubMed]
118. Joaquim, D.C.; Borges, E.D.; Viana, I.G.R.; Navarro, P.A.; Vireque, A.A. Risk of Contamination of Gametes and Embryos during Cryopreservation and Measures to Prevent Cross-Contamination. *BioMed Res. Int.* **2017**, *2017*, 1840417. [CrossRef] [PubMed]
119. dos Santos Neto, P.C.; Vilariño, M.; Barrera, N.; Cuadro, F.; Crispo, M.; Menchaca, A. Cryotolerance of Day 2 or Day 6 in Vitro Produced Ovine Embryos after Vitrification by Cryotop or Spatula Methods. *Cryobiology* **2015**, *70*, 17–22. [CrossRef]
120. Oliveira, C.S.; Feuchard, V.L.d.S.; de Freitas, C.; Rosa, P.M.d.S.; Camargo, A.J.d.R.; Saraiva, N.Z. In-Straw Warming Protocol Improves Survival of Vitrified Embryos and Allows Direct Transfer in Cattle. *Cryobiology* **2020**, *97*, 222–225. [CrossRef]
121. Bottrel, M.; Mogas, T.; Pereira, B.; Ortiz, I.; Díaz-Jiménez, M.; Consuegra, C.; Hidalgo, M.; Morató, R.; Dorado, J. The Cryoprotective Effect of Ficoll 70 on the Post-Warming Survival and Quality of Cryotop-Vitrified Donkey Embryos: Vitrifying Donkey Embryos with Ficoll. *Theriogenology* **2020**, *148*, 180–185. [CrossRef]

122. Somfai, T.; Hirao, Y. Vitrification of Immature Bovine Oocytes in Protein-Free Media: The Impact of the Cryoprotectant Treatment Protocol, Base Medium, and Ovary Storage. *Theriogenology* **2021**, *172*, 47–54. [CrossRef]
123. Seki, S.; Basaki, K.; Komatsu, Y.; Fukuda, Y.; Yano, M.; Matsuo, Y.; Obata, T.; Matsuda, Y.; Nishijima, K. Vitrification of One-Cell Mouse Embryos in Cryotubes. *Cryobiology* **2018**, *81*, 132–137. [CrossRef] [PubMed]
124. Amorim, C.A.; David, A.; Van Langendonckt, A.; Dolmans, M.M.; Donnez, J. Vitrification of Human Ovarian Tissue: Effect of Different Solutions and Procedures. *Fertil. Steril.* **2011**, *95*, 1094–1097. [CrossRef] [PubMed]
125. El-Sharawy, M.E.; Almadaly, E.A.; El-Domany, W.B.; Essawy, M.M.; Shamiah, S.M.; El-Shamaa, I.S.; Zaghloul, H.K. Ultrastructural Changes in Immature Ovine Cumulus-Oocyte Complexes Vitrified in Conventional and Open Pulled Straws. *Small Rumin. Res.* **2021**, *199*, 106367. [CrossRef]
126. Kornienko, E.V.; Romanova, A.B.; Ikonopistseva, M.V.; Malenko, G.P. Optimization of Triacetate Cellulose Hollow Fiber Vitrification (HFV) Method for Cryopreservation of in Vitro Matured Bovine Oocytes. *Cryobiology* **2020**, *97*, 66–70. [CrossRef]
127. Sugiyama, R.; Nakagawa, K.; Shirai, A.; Sugiyama, R.; Nishi, Y.; Kuribayashi, Y.; Inoue, M. Clinical Outcomes Resulting from the Transfer of Vitrified Human Embryos Using a New Device for Cryopreservation (Plastic Blade). *J. Assist. Reprod. Genet.* **2010**, *27*, 161–167. [CrossRef]
128. Nakayama, K.; Chinen, S.; Teshima, J.; Tamada, Y.; Hirabayashi, M.; Hochi, S. Silk Fibroin Sheet Multilayer Suitable for Vitrification of in Vitro-Matured Bovine Oocytes. *Theriogenology* **2020**, *145*, 109–114. [CrossRef]
129. Hayashi, A.; Maehara, M.; Uchikura, A.; Matsunari, H.; Matsumura, K.; Hyon, S.H.; Sato, M.; Nagashima, H. Development of an Efficient Vitrification Method for Chondrocyte Sheets for Clinical Application. *Regen. Ther.* **2020**, *14*, 215–221. [CrossRef]
130. Xiao, Z.; Wang, Y.; Li, L.; Luo, S.; Li, S.W. Needle Immersed Vitrification Can Lower the Concentration of Cryoprotectant in Human Ovarian Tissue Cryopreservation. *Fertil. Steril.* **2010**, *94*, 2323–2328. [CrossRef]
131. Zhou, X.H.; Wu, Y.J.; Shi, J.; Xia, Y.; Zheng, S. Sen. Cryopreservation of Human Ovarian Tissue: Comparison of Novel Direct Cover Vitrification and Conventional Vitrification. *Cryobiology* **2010**, *60*, 101–105. [CrossRef]
132. Bebbere, D.; Pinna, S.; Nieddu, S.; Natan, D.; Arav, A.; Ledda, S. Gene Expression Analysis of Ovine Prepubertal Testicular Tissue Vitrified with a Novel Cryodevice (E.Vit). *J. Assist. Reprod. Genet.* **2019**, *36*, 2145–2154. [CrossRef]
133. Rahimi, G.; Isachenko, V.; Kreienberg, R.; Sauer, H.; Todorov, P.; Tawadros, S.; Mallmann, P.; Nawroth, F.; Isachenko, E. Re-Vascularisation in Human Ovarian Tissue after Conventional Freezing or Vitrification and Xenotransplantation. *Eur. J. Obstet. Gynecol. Reprod. Biol.* **2010**, *149*, 63–67. [CrossRef] [PubMed]
134. Lima, D.B.C.; Da Silva, L.D.M.; Comizzoli, P. Influence of Warming and Reanimation Conditions on Seminiferous Tubule Morphology, Mitochondrial Activity, and Cell Composition of Vitrified Testicular Tissues in the Domestic Cat Model. *PLoS ONE* **2018**, *13*, e0207317. [CrossRef] [PubMed]
135. Ramezani, M.; Salehnia, M.; Jafarabadi, M. Vitrification and in Vitro Culture Had No Adverse Effect on the Follicular Development and Gene Expression of Stimulated Human Ovarian Tissue. *J. Obstet. Gynaecol. Res.* **2018**, *44*, 474–487. [CrossRef] [PubMed]
136. Yamini, N.; Pourmand, G.; Amidi, F.; Salehnia, M.; Nejad, N.A.; Mougahi, S.M.H.N. Developmental Potential of Vitrified Mouse Testicular Tissue after Ectopic Transplantation. *Cell J.* **2016**, *18*, 74–82. [CrossRef]
137. Fujihara, M.; Kaneko, T.; Inoue-Murayama, M. Vitrification of Canine Ovarian Tissues with Polyvinylpyrrolidone Preserves the Survival and Developmental Capacity of Primordial Follicles. *Sci. Rep.* **2019**, *9*, 3970. [CrossRef]
138. Benvenutti, L.; Salvador, R.A.; Til, D.; Senn, A.P.; Tames, D.R.; Amaral, N.L.L.; Amaral, V.L.L. Wistar Rats Immature Testicular Tissue Vitrification and Heterotopigrafting. *J. Bras. De Reprod. Assist.* **2018**, *22*, 167–173. [CrossRef]
139. Xu, H.; Shi, H.; Zang, W.-F.; Lu, D. An Experimental Research on Cryopreserving Rabbit Trachea by Vitrification. *Cryobiology* **2009**, *58*, 225–231. [CrossRef]
140. de Graaf, I.A.M.; Draaisma, A.L.; Schoeman, O.; Fahy, G.M.; Groothuis, G.M.M.; Koster, H.J. Cryopreservation of Rat Precision-Cut Liver and Kidney Slices by Rapid Freezing and Vitrification. *Cryobiology* **2007**, *54*, 1–12. [CrossRef]
141. Jomha, N.M.; Elliott, J.A.W.; Law, G.K.; Maghdoori, B.; Fraser Forbes, J.; Abazari, A.; Adesida, A.B.; Laouar, L.; Zhou, X.; McGann, L.E. Vitrification of Intact Human Articular Cartilage. *Biomaterials* **2012**, *33*, 6061–6068. [CrossRef]
142. Wu, K.; Shardt, N.; Laouar, L.; Chen, Z.; Prasad, V.; Elliott, J.A.W.; Jomha, N.M. Comparison of Three Multi-Cryoprotectant Loading Protocols for Vitrification of Porcine Articular Cartilage. *Cryobiology* **2020**, *92*, 151–160. [CrossRef]
143. Aertsen, A.; Meersman, F.; Hendrickx, M.E.G.; Vogel, R.F.; Michiels, C.W. Biotechnology under High Pressure: Applications and Implications. *Trends Biotechnol.* **2009**, *27*, 434–441. [CrossRef] [PubMed]
144. De Heer, J. The Principle of Le Châtelier and Braun. *J. Chem. Educ.* **1957**, *34*, 375–380. [CrossRef]
145. Meersman, F.; Dobson, C.M.; Heremans, K. Protein Unfolding, Amyloid Fibril Formation and Configurational Energy Landscapes under High Pressure Conditions. *Chem. Soc. Rev.* **2006**, *35*, 908–917. [CrossRef]
146. Silva, J.L.; Foguel, D.; Royer, C.A. Pressure Provides New Insights into Protein Folding, Dynamics and Structure. *Trends Biochem. Sci.* **2001**, *26*, 612–618. [CrossRef]
147. Shung, K.K.; Krisko, B.A.; Ballard, J.O. Acoustic Measurement of Erythrocyte Compressibility. *J. Acoust. Soc. Am.* **1982**, *72*, 1364–1367. [CrossRef]
148. Hall, A.C.; Pickles, D.M.; Macdonald, A.G. Advances in Comparative and Enviromental Physiology. In *Advances in Comparative and Enviromental Physiology*; Macdonald, A.G., Ed.; Springer: Berlin, Germany, 1993; p. 17.

149. Lammi, M.J.; Hakkinen, T.P.; Parkkinen, J.J.; Hyttinen, M.M.; Jortikka, M.; Helminen, H.J.; Tammi, M.I. Adaptation of Canine Femoral Head Articular Cartilage to Long Distance Running Exercise in Young Beagles. *Ann. Rheum. Dis.* **1993**, *52*, 369–377. [CrossRef]
150. Marsland, D. Cells at High Pressure. *Sci. Am.* **1958**, *199*, 36–43. [CrossRef]
151. Zimmerman, A.M.; Marsland, D. Cell Division: Effects of Pressure on the Mitotic Mechanisms of Marine Eggs (Arbacia Punctulata). *Exp. Cell Res.* **1964**, *35*, 293–302. [CrossRef]
152. Forer, A.; Zimmerman, A.M. Spindle Birefringence of Isolated Mitotic Apparatus Analysed by Treatments with Cold, Pressure, and Diluted Isolation Medium. *J. Cell Sci.* **1976**, *20*, 329–339. [CrossRef]
153. Bourns, B.; Franklin, S.; Cassimeris, L.; Salmon, E.D. High Hydrostatic Pressure Effects in Vivo: Changes in Cell Morphology, Microtubule Assembly, and Actin Organization. *Cell Motil. Cytoskelet.* **1988**, *10*, 380–390. [CrossRef] [PubMed]
154. Symington, A.L.; Zimmerman, S.; Stein, J.; Stein, G.; Zimmerman, A.M. Hydrostatic Pressure Influences Histone MRNA. *J. Cell Sci.* **1991**, *98*, 123–129. [CrossRef] [PubMed]
155. Haskin, C.; Cameron, I. Physiological Levels of Hydrostatic Pressure Alter Morphology and Organization of Cytoskeletal and Adhesion Proteins in MG-63 Osteosarcoma Cells. *Biochem. Cell Biol. Biochim. Et Biol. Cell* **1993**, *71*, 27–35. [CrossRef] [PubMed]
156. Haskin, C.L.; Athanasiou, K.A.; Klebe, R.; Cameron, I.L. A Heat-Shock-like Response with Cytoskeletal Disruption Occurs Following Hydrostatic Pressure in MG-63 Osteosarcoma Cells. *Biochem. Cell Biol.* **1993**, *71*, 361–371. [CrossRef] [PubMed]
157. Wilson, R.G.; Trogadis, J.E.; Zimmerman, S.; Zimmerman, A.M. Hydrostatic Pressure Induced Changes in the Cytoarchitecture of Pheochromocytoma (PC-12) Cells. *Cell Biol. Int.* **2001**, *25*, 649–666. [CrossRef] [PubMed]
158. Wilson, R.G.; Zimmerman, S.; Zimmerman, A.M. The Effects of Hydrostatic Pressure-Induced Changes on the Cytoskeleton and on the Regulation of Gene Expression in Pheochromocytoma (PC-12) Cells. *Cell Biol. Int.* **2001**, *25*, 667–677. [CrossRef]
159. Karow, A.M.; Liu, W.P.; Humphries, A.L. Survival of Dog Kidneys Subjected to High Pressures: Necrosis of Kidneys after Freezing. *Cryobiology* **1970**, *7*, 122–128. [CrossRef]
160. Fahy, G.M. The Biophysics of Organ Cryopreservation. In *The Biophysics of Organ Cryopreservation*; Peggy, D.E., Karow, A., Eds.; Plenum: New York, NY, USA, 1987; p. 339.
161. Frey, B.; Janko, C.; Ebel, N.; Meister, S.; Schlucker, E.; Meyer-Pittroff, R.; Fietkau, R.; Herrmann, M.; Gaipl, U. Cells Under Pressure—Treatment of Eukaryotic Cells with High Hydrostatic Pressure, from Physiologic Aspects to Pressure Induced Cell Death. *Curr. Med. Chem.* **2008**, *15*, 2329–2336. [CrossRef]
162. Multhoff, G. Heat Shock Protein 70 (Hsp70): Membrane Location, Export and Immunological Relevance. *Methods* **2007**, *43*, 229–237. [CrossRef]
163. Kaarniranta, K.; Elo, M.; Sironen, R.; Lammi, M.J.; Goldring, M.B.; Eriksson, J.E.; Sistonen, L.; Helminen, H.J. Hsp70 Accumulation in Chondrocytic Cells Exposed to High Continuous Hydrostatic Pressure Coincides with MRNA Stabilization Rather than Transcriptional Activation. *Proc. Natl. Acad. Sci. USA* **2002**, *95*, 2319–2324. [CrossRef]
164. Kaarniranta, K.; Elo, M.A.; Sironen, R.K.; Karjalainen, H.M.; Helminen, H.J.; Lammi, M.J. Stress Responses of Mammalian Cells to High Hydrostatic Pressure. *Biorheology* **2002**, *40*, 87–92.
165. Kaarniranta, K.; Holmberg, C.I.; Lammi, M.J.; Eriksson, J.E.; Sistonen, L.; Helminen, H.J. Primary Chondrocytes Resist Hydrostatic Pressure-Induced Stress While Primary Synovial Cells and Fibroblasts Show Modified Hsp70 Response. *Osteoarthr. Cartil.* **2001**, *9*, 7–13. [CrossRef] [PubMed]
166. Islam, N.; Haqqi, T.M.; Jepsen, K.J.; Kraay, M.; Welter, J.F.; Goldberg, V.M.; Malemud, C.J. Hydrostatic Pressure Induces Apoptosis in Human Chondrocytes from Osteoarthritic Cartilage through Up-Regulation of Tumor Necrosis Factor-α, Inducible Nitric Oxide Synthase, P53, c-Myc, and Bax-α, and Suppression of Bcl-2. *J. Cell. Biochem.* **2000**, *87*, 266–278. [CrossRef] [PubMed]
167. Boonyaratanakornkit, B.B.; Park, C.B.; Clark, D.S. Pressure Effects on Intra- and Intermolecular Interactions within Proteins. *Biochim. Et Biophys. Acta-Protein Struct. Mol. Enzymol.* **2002**, *1595*, 235–249. [CrossRef]
168. Heremans, K. High Pressure Effects on Proteins and Other Biomolecules. *Annu. Rev. Biophys. Bioeng.* **1982**, *11*, 1–21. [CrossRef]
169. Heremans, K.; Smeller, L. Protein Structure and Dynamics at High Pressure1. *Biochim. Et Biophys. Acta-Protein Struct. Mol. Enzymol.* **1998**, *1386*, 353–370. [CrossRef] [PubMed]
170. Winter, R.; Dzwolak, W.; Wolynes, P.G.; Dobson, C.M.; Saykally, R.J. Exploring the Temperature-Pressure Configurational Landscape of Biomolecules: From Lipid Membranes to Proteins. *Philos. Trans. R. Soc. A Math. Phys. Eng. Sci.* **2005**, *363*, 537–563. [CrossRef]
171. Meersman, F.; Smeller, L.; Heremans, K. Protein Stability and Dynamics in the Pressure-Temperature Plane. *Biochim. Et Biophys. Acta-Proteins Proteom.* **2006**, *1764*, 346–354. [CrossRef]
172. Winter, R.; Dzwolak, W. Temperature-Pressure Configurational Landscape of Lipid Bilayers and Proteins. *Cell. Mol. Biol.* **2004**, *50*, 397–417.
173. Balny, C.; Hayashi, R. *High Pressure Bioscience and Biotechnology*, 1st ed.; Elsevier Science B.V.: Amsterdam, The Netherlands, 1996.
174. Balny, C. *Advances in High Pressure Bioscience and Biotechnology*; Ludwig, H., Ed.; Springer: Berlin, Germany, 1999.
175. Balny, C.; Masson, P.; Heremans, K. High Pressure Effects on Biological Macromolecules: From Structural Changes to Alteration of Cellular Processes. *Biochim. Et Biophys. Acta* **2002**, *1595*, 3–10. [CrossRef]
176. Smeller, L.; Meersman, F.; Heremans, K. Refolding Studies Using Pressure: The Folding Landscape of Lysozyme in the Pressure–Temperature Plane. *Biochim. Et Biophys. Acta (Bba)-Proteins Proteom.* **2006**, *1764*, 497–505. [CrossRef]

177. Winter, R. Synchrotron X-Ray and Neutron Small-Angle Scattering of Lyotropic Lipid Mesophases, Model Biomembranes and Proteins in Solution at High Pressure. *Biochim. Et Biophys. Acta (Bba)-Protein Struct. Mol. Enzymol.* **2002**, *1595*, 160–184. [CrossRef]
178. Smeller, L. The Pressure Dependence of the Lipid Phase Transitions. Effect of the Pressure on the Pre-and Subtransition. *J. Theor. Biol.* **1990**, *142*, 453–462. [CrossRef] [PubMed]
179. Take, J.; Yamaguchi, T.; Mine, N.; Terada, S. Caspase Activation in High-Pressure. Induced Apoptosis of Murine Erythroleukemia Cells. *Jpn. J. Physiol.* **2005**, *51*, 193–199. [CrossRef] [PubMed]
180. Yamaguchi, T.; Hashiguchi, K.; Katsuki, S.; Iwamoto, W.; Tsuruhara, S.; Terada, S. Activation of the Intrinsic and Extrinsic Pathways in High Pressure-Induced Apoptosis of Murine Erythroleukemia Cells. *Cell. Mol. Biol. Lett.* **2008**, *13*, 49–57. [CrossRef]
181. Diehl, P.; Schmitt, M.; Blümelhuber, G.; Frey, B.; Van Laak, S.; Fischer, S.; Muehlenweg, B.; Meyer-Pittroff, R.; Gollwitzer, H.; Mittelmeier, W. Induction of Tumor Cell Death by High Hydrostatic Pressure as a Novel Supporting Technique in Orthopedic Surgery. *Oncol. Rep.* **2003**, *10*, 1851–1855. [CrossRef] [PubMed]
182. Frey, B.; Franz, S.; Sheriff, A.; Korn, A.; Bluemelhuber, G.; Gaipl, U.S.; Voll, R.E.; Meyer-Pittroff, R.; Herrmann, M. Hydrostatic Pressure Induced Death of Mammalian Cells Engages Pathways Related to Apoptosis or Necrosis. *Cell. Mol. Biol.* **2004**, *50*, 459–467.
183. Korn, A.; Frey, B.; Sheriff, A.; Gaipl, U.S.; Franz, S.; Meyer-Pttroff, R.; Herrmann, M.; Bluemelhuber, G. High Hydrostatic Pressure Inactivated Human Tumour Cells Preserve Their Immunogenicity. *Cell. Mol. Biol.* **2004**, *50*, 65–74.
184. Takano, T.; Yamanquchi, Y.; Satou, T.; Takano, K.J. Pressure-Induced Cell Death and Apoptosis in Human Lymphoblasts. *Jpn. J. Hum. Genet.* **1997**, *42*, 111.
185. Frey, B.; Hartmann, M.; Herrmann, M.; Meyer-Pittroff, R.; Sommer, K.; Bluemelhuber, G. Microscopy under Pressure—An Optical Chamber System for Fluorescence Microscopic Analysis of Living Cells under High Hydrostatic Pressure. *Microsc. Res. Tech.* **2006**, *69*, 65–72. [CrossRef]
186. Hartmann, M.; Pfeifer, F.; Dornheim, G.; Sommer, K. High Pressure Cell for Observing Microscopic Processes under High Pressure. *Chem.-Ing.-Tech.* **2003**, *75*, 1763–1767. [CrossRef]
187. Hartmann, M.; Kreuss, M.; Sommer, K. High Pressure Microscopy–a Powerful Tool for Monitoring Cells and Macromolecules under High Hydrostatic Pressure. *Cell. Mol. Biol.* **2004**, *50*, 479–484. [PubMed]
188. Pegg, D. Principles of Cryopreservation. *Methods Mol Biol* **2007**, *368*, 39–57. [PubMed]
189. Fahy, G.M.; Wowk, B. Principles of Cryopreservation by Vitrification. *Methods Mol. Biol.* **2015**, *1257*, 21–82. [CrossRef] [PubMed]
190. Weng, L.; Stott, S.L.; Toner, M. Exploring Dynamics and Structure of Biomolecules, Cryoprotectants, and Water Using Molecular Dynamics Simulations: Implications for Biostabilization and Biopreservation. *Annu. Rev. Biomed. Eng.* **2018**, *21*, 1–31. [CrossRef] [PubMed]
191. Towey, J.J.; Dougan, L. Structural Examination of the Impact of Glycerol on Water Structure. *J. Phys. Chem. B* **2012**, *116*, 1633–1641. [CrossRef] [PubMed]
192. Weng, L.; Ziaei, S.; Elliott, G.D. Effects of Water on Structure and Dynamics of Trehalose Glasses at Low Water Contents and Its Relationship to Preservation Outcomes. *Sci. Rep.* **2016**, *6*, 28795. [CrossRef]
193. Egorov, A.V.; Lyubartsev, A.P.; Laaksonen, A. Molecular Dynamics Simulation Study of Glycerol-Water Liquid Mixtures. *J. Phys. Chemistry. B* **2011**, *115*, 14572–14581. [CrossRef]
194. Weng, L.; Elliott, G.D. Dynamic and Thermodynamic Characteristics Associated with the Glass Transition of Amorphous Trehalose-Water Mixtures. *Phys. Chem. Chem. Phys. Pccp* **2014**, *16*, 11555–11565. [CrossRef]
195. Conrad, P.B.; de Pablo, J.J. Computer Simulation of the Cryoprotectant Disaccharide α,α-Trehalose in Aqueous Solution. *J. Phys. Chem. A* **1999**, *103*, 4049–4055. [CrossRef]
196. Lerbret, A.; Bordat, P.; Affouard, F.; Descamps, M.; Migliardo, F. How Homogeneous Are the Trehalose, Maltose, and Sucrose Water Solutions? An Insight from Molecular Dynamics Simulations. *J. Phys. Chemistry. B* **2005**, *109*, 11046–11057. [CrossRef]
197. Fahy, G.M. The Relevance of Cryoprotectant "Toxicity" to Cryobiology. *Cryobiology* **1986**, *23*, 1–13. [CrossRef] [PubMed]
198. Fahy, G.M.; Levy, D.I.; Ali, S.E. Some Emerging Principles Underlying the Physical Properties, Biological Actions, and Utility of Vitrification Solutions. *Cryobiology* **1987**, *24*, 196–213. [CrossRef] [PubMed]
199. Abazari, A.; Jomha, N.M.; Elliott, J.A.W.; McGann, L.E. Cryopreservation of Articular Cartilage. *Cryobiology* **2013**, *66*, 201–209. [CrossRef]
200. Naccache, P. Patterns of Nonelectrolyte Permeability in Human Red Blood Cell Membrane. *J. Gen. Physiol.* **1973**, *62*, 714–736. [CrossRef] [PubMed]
201. Sum, A.K.; Faller, R.; De Pablo, J.J. Molecular Simulation Study of Phospholipid Bilayers and Insights of the Interactions with Disaccharides. *Biophys. J.* **2003**, *85*, 2830–2844. [CrossRef] [PubMed]
202. Pereira, C.S.; Lins, R.D.; Chandrasekhar, I.; Freitas, L.C.G.; Hünenberger, P.H. Interaction of the Disaccharide Trehalose with a Phospholipid Bilayer: A Molecular Dynamics Study. *Biophys. J.* **2004**, *86*, 2273–2285. [CrossRef] [PubMed]
203. Pereira, C.S.; Hünenberger, P.H. Interaction of the Sugars Trehalose, Maltose and Glucose with a Phospholipid Bilayer: A Comparative Molecular Dynamics Study. *J. Phys. Chem. B* **2006**, *110*, 15572–15581. [CrossRef]
204. Hughes, Z.E.; Malajczuk, C.J.; Mancera, R.L. The Effects of Cryosolvents on DOPC-β-Sitosterol Bilayers Determined from Molecular Dynamics Simulations. *J. Phys. Chem. B* **2013**, *117*, 3362–3375. [CrossRef]

205. Malajczuk, C.J.; Hughes, Z.E.; Mancera, R.L. Molecular Dynamics Simulations of the Interactions of DMSO, Mono- and Polyhydroxylated Cryosolvents with a Hydrated Phospholipid Bilayer. *Biochim. Et Biophys. Acta-Biomembr.* **2013**, *1828*, 2041–2055. [CrossRef]
206. Notman, R.; Noro, M.; O'Malley, B.; Anwar, J. Molecular Basis for Dimethylsulfoxide (DMSO) Action on Lipid Membranes. *J. Am. Chem. Soc.* **2006**, *128*, 13982–13983. [CrossRef]
207. Gurtovenko, A.A.; Anwar, J. Modulating the Structure and Properties of Cell Membranes: The Molecular Mechanism of Action of Dimethyl Sulfoxide. *J. Phys. Chem. B* **2007**, *111*, 10453–10460. [CrossRef] [PubMed]
208. Hughes, Z.E.; Mark, A.E.; Mancera, R.L. Molecular Dynamics Simulations of the Interactions of DMSO with DPPC and DOPC Phospholipid Membranes. *J. Phys. Chem. B* **2012**, *116*, 11911–11923. [CrossRef] [PubMed]
209. Warner, R.M.; Ampo, E.; Nelson, D.; Benson, J.D.; Eroglu, A.; Higgins, A.Z. Rapid Quantification of Multi-Cryoprotectant Toxicity Using an Automated Liquid Handling Method. *Cryobiology* **2021**, *98*, 219–232. [CrossRef] [PubMed]
210. Benson, J.D.; Higgins, A.Z.; Desai, K.; Eroglu, A. A Toxicity Cost Function Approach to Optimal CPA Equilibration in Tissues. *Cryobiology* **2018**, *80*, 144–155. [CrossRef]
211. Benson, J.D.; Kearsley, A.J.; Higgins, A.Z. Mathematical Optimization of Procedures for Cryoprotectant Equilibration Using a Toxicity Cost Function. *Cryobiology* **2012**, *64*, 144–151. [CrossRef]
212. Glick, D.; Malmstrom, B.G. Studies in Histochemistry XXIII. Simple and Efficient Freezing-Drying Apparatus for the Preparation of Embedded Tissue. *Exp. Cell Res.* **1952**, *3*, 125–135. [CrossRef]
213. REBHUN, L.I. Applications of Freeze-Substitution to Electron Microscope Studies of Invertebrate Oocytes. *J. Biophys. Biochem. Cytol.* **1961**, *9*, 785–798. [CrossRef]
214. Rick, R.; Dörge, A.; Thurau, K. Quantitative Analysis of Electrolytes in Frozen Dried Sections. *J. Microsc.* **1982**, *125*, 239–247. [CrossRef]
215. Steinbrecht, R.A. Cryofixation without Cryoprotectants. Freeze Substitution and Freeze Etching of an Insect Olfactory Receptor. *Tissue Cell* **1980**, *12*, 73–100. [CrossRef]
216. Steinbrecht, R.A. Experiments on Freezing Damage with Freeze Substitution Using Moth Antennae as Test Objects. *J. Microsc.* **1982**, *125*, 187–192. [CrossRef]
217. Porter, K.R.; Anderson, K.L. The Structure of the Cytoplasmic Matrix Preserved by Freeze-Drying and Freeze-Substitution. *Eur. J. Cell Biol.* **1982**, *29*, 83–96. [PubMed]
218. Silvester, N.R.; Marchese-Ragona, S.; Johnston, D.N. The Relative Efficiency of Various Fluids in the Rapid Freezing of Protozoa. *J. Microsc.* **1982**, *128*, 175–186. [CrossRef] [PubMed]
219. Severs, N. *Rapid Freezing of Unpretreated Tissues for Freeze-Fracture Electron Microscopy*; Wiley-Liss: New York, NY, USA, 1983.
220. Moor, H.; Mühletttaler, K. Fine Structure in Frozen-Etched Yeast Cells. *J. Cell Biol.* **1963**, *17*, 609–628. [CrossRef]
221. Bank, H.; Mazur, P. Visualization of Freezing Damage. *J. Cell Biol.* **1973**, *57*, 729–742. [CrossRef]
222. Howard, R.J.; Aist, J.R. Hyphal Tip Cell Ultrastructure of the Fungus Fusarium: Improved Preservation by Freeze-Substitution. *J. Ultrasructure Res.* **1979**, *66*, 224–234. [CrossRef] [PubMed]
223. Howard, R.J.; Aist, J.R. Cytoplasmic Microtubules and Fungal Morphogenesis: Ultrastructural Effects of Methyl Benzimidazole-2-Ylcarbamate Determined by Freeze-Substitution of Hyphal Tip Cells. *J. Cell Biol.* **1980**, *87*, 55–64. [CrossRef]
224. Allen, N.S. Cytoplasmic Streaming and Transport in the Characean Alga *Nitella*. *Can. J. Bot.* **1980**, *58*, 786–796. [CrossRef]
225. Hoch, H.C.; Howard, R.J. Ultrastructure of Freeze-Substituted Hyphae of the Basidiomycete Laetisaria Arvalis. *Protoplasma* **1980**, *103*, 281–297. [CrossRef]
226. Gupta, B.L.; Hall, T.A. The X-Ray Microanalysis of Frozen-Hydrated Sections in Scanning Electron Microscopy: An Evaluation. *Tissue Cell* **1981**, *13*, 623–643. [CrossRef]
227. Howard, R.J. Ultrastructural Analysis of Hyphal Tip Cell Growth in Fungi: Spitzenkorper, Cytoskeleton and Endomembranes after Freeze-Substitution. *J. Cell Sci.* **1981**, *48*, 89–103. [CrossRef]
228. Handley, D.A.; Alexander, J.T.; Chien, S. The Design and Use of a Simple Device for Rapid Quench-freezing of Biological Samples. *J. Microsc.* **1981**, *121*, 273–282. [CrossRef] [PubMed]
229. Bellare, J.R.; Davis, H.T.; Scriven, L.E.; Talmon, Y. Controlled Environment Vitrification System: An Improved Sample Preparation Technique. *J. Electron Microsc. Tech.* **1988**, *10*, 87–111. [CrossRef] [PubMed]
230. Ryan, K.P.; Purse, D.H.; Robinson, S.G.; Wood, J.W. The Relative Efficiency of Cryogens Used for Plunge-Cooling Biological Specimens. *J. Microsc.* **1987**, *145*, 89–96. [CrossRef] [PubMed]
231. Glover, A.J.; Garvitch, Z.S. The Freezing Rate of Freeze-Etch Specimens for Electron Microscopy. *Cryobiology* **1974**, *11*, 248–254. [CrossRef]
232. Escaig, J. New Instruments Which Facilitate Rapid Freezing at 83 K and 6 K. *J. Microsc.* **1982**, *126*, 221–229. [CrossRef]
233. Heath, I.B.; Rethoret, K. Mitosis in the Fungus Zygorhynchus Moelleri: Evidence for Stage Specific Enhancement of Microtubule Preservation by Freeze Substitution. *Eur. J. Cell. Biol.* **1982**, *28*, 180–189.
234. Costello, M.J.; Corless, J.M. The Direct Measurement of Temperature Changes within Freeze-fracture Specimens during Rapid Quenching in Liquid Coolants. *J. Microsc.* **1978**, *112*, 17–37. [CrossRef]
235. Schwabe, K.G.; Terracio, L. Ultrastructural and Thermocouple Evaluation of Rapid Freezing Techniques. *Cryobiology* **1980**, *17*, 571–584. [CrossRef]

236. Marchese-Ragona, S.P. Ethanol, an Efficient Coolant for Rapid Freezing of Biological Material. *J. Microsc.* **1984**, *134*, 169–171. [CrossRef]
237. Steinbrecht, R.A.; Zierold, K. A Cryoembedding Method for Cutting Ultrathin Cryosections from Small Frozen Specimens. *J. Microsc.* **1984**, *136*, 69–75. [CrossRef]
238. Lee, H.N.; Park, J.K.; Paek, S.K.; Byun, J.H.; Song, H.; Lee, H.J.; Chang, E.M.; Kim, J.W.; Lee, W.S.; Lyu, S.W. Does Duration of Cryostorage Affect Survival Rate, Pregnancy, and Neonatal Outcomes? Large-Scale Single-Center Study of Slush Nitrogen (SN2) Vitrified-Warmed Blastocysts. *Int. J. Gynecol. Obstet.* **2021**, *152*, 351–357. [CrossRef] [PubMed]
239. Osman, E.K.; Esbert, M.; Hanson, B.M.; Winslow, A.D.; Seli, E.; Scott, R.T. EMBRYO VITRIFICATION IN SUPER COOLED SLUSH NITROGEN RESULTS IN SUPERIOR POST-THAW SURVIVAL COMPARED TO CONVENTIONAL LIQUID NITROGEN: A BLINDED, RANDOMIZED CONTROLLED TRIAL. *Fertil. Steril.* **2020**, *114*, e38. [CrossRef]
240. Ryan, K.P.; Liddicoat, M.I. Safety Considerations Regarding the Use of Propane and Other Liquefied Gases as Coolants for Rapid Freezing Purposes. *J. Microsc.* **1987**, *147*, 337–340. [CrossRef] [PubMed]
241. Mueller, M.; Meister, N.; Moor, H. Freezing in a Propane Jet and Its Application in Freeze-Fracturing. *Mikroskopie* **1980**, *36*, 129–140.
242. Greene, W.B.; Walsh, L.G. An Improved Cryo-Jet Freezing Method. *J. Microsc.* **1992**, *166*, 207–218. [CrossRef]
243. Knoll, G.; Oebel, G.; Plattner, H. A Simple Sandwich-Cryogen-Jet Procedure with High Cooling Rates for Cryofixation of Biological Materials in the Native State. *Protoplasma* **1982**, *111*, 161–176. [CrossRef]
244. Pscheid, P.; Schudt, C.; Plattner, H. Cryofixation of Monolayer Cell Cultures for Freeze-Fracturing without Chemical Pre-Treatments. *J. Microsc.* **1981**, *121*, 149–167. [CrossRef]
245. Boyne, A. A Gentle, Bounce-Free Assembly for Quick-Freezing Tissues for Electron Microscopy: Application to Isolated Torpedine Ray Electrocyte Stacks. *J. Neurosci. Methods* **1979**, *1*, 353–364. [CrossRef]
246. Heuser, J.; Reese, T.; Dennis, M.; Jan, Y. Synaptic Vesicle Exocytosis Captured by Quick Freezing and Correlated with Quantal Transmitter Release. *J. Cell Biol.* **1979**, *81*, 275. [CrossRef]
247. Heuser, J.; Reese, T.; Landis, D. Preservation of Synaptic Structure by Rapid Freezing. *Cold Spring Harb Symp Quant Biol* **1976**, *40*, 17–24. [CrossRef]
248. Simpson, W.L. An Experimental Analysis of the Altmann Technic of Freezing-Drying. *Anat. Rec.* **1941**, *80*, 173–189. [CrossRef]
249. van Harreveld, A.; Crowell, J. Electron Microscopy after Rapid Freezing on a Metal Surface and Substitution Fixation. *Anat. Rec.* **1964**, *149*, 381–385. [CrossRef] [PubMed]
250. Van Harreveld, A.; Crowell, J.; Malhotra, S. A Study of Extracellular Space in Central Nervous Tissue by Freeze-Substitution. *J. Cell Biol.* **1965**, *25*, 117. [CrossRef] [PubMed]
251. Phillips, T.E.; Boyne, A.F. Liquid Nitrogen-based Quick Freezing: Experiences with Bounce-free Delivery of Cholinergic Nerve Terminals to a Metal Surface. *J. Electron Microsc. Tech.* **1984**, *1*, 9–29. [CrossRef]
252. Heath, I.B. A Simple and Inexpensive Liquid Helium Cooled 'Slam Freezing' Device. *J. Microsc.* **1984**, *135*, 75–82. [CrossRef]
253. Hirokawa, N.; Kirino, T. An Ultrastructural Study of Nerve and Glial Cells by Freeze-Substitution. *J. Neurocytol.* **1980**, *9*, 243–254. [CrossRef]
254. Ichikawa, A.; Ichikawa, M.; Hirokawa, N. The Ultrastructure of Rapid-frozen, Substitution Fixed Parotid Gland Acinar Cells of the Mongolian Gerbil (Meriones Meridianus). *Am. J. Anat.* **1980**, *157*, 107–110. [CrossRef]
255. Ornberg, R.; Reese, T. A Freeze-Substitution Method for Localizing Divalent Cations: Examples from Secretory Systems. *europepmc.org* **1980**, *3*, 2802–2808.
256. Hirokawa, N.; Heuser, J. Quick-Freeze, Deep-Etch Visualization of the Cytoskeleton beneath Surface Differentiations of Intestinal Epithelial Cells. *J. Cell Biol.* **1981**, *91*, 399. [CrossRef]
257. Terracio, L.; Bankston, P.; McAteer, J. Ultrastructural Observations on Tissues Processed by a Quick-Freezing, Rapid-Drying Method: Comparison with Conventional Specimen Preparation. *Elsevier* **1981**, *18*, 55–71. [CrossRef]
258. Hirokawa, N. Cross-Linker System between Neurofilaments, Microtubules and Membranous Organelles in Frog Axons Revealed by the Quick-Freeze, Deep-Etching Method. *J. Cell Biol.* **1982**, *94*, 129. [CrossRef] [PubMed]
259. Schnapp, B.; Reese, T. Cytoplasmic Structure in Rapid-Frozen Axons. *J. Cell Biol.* **1982**, *94*, 667. [CrossRef] [PubMed]
260. McGuire, P.G.; Twietmeyer, T.A. Morphology of Rapidly Frozen Aortic Endothelial Cells. Glutaraldehyde Fixation Increases the Number of Caveolae. *Circ. Res.* **1983**, *53*, 424–429. [CrossRef] [PubMed]
261. Menco, B.P.M. Ciliated and Microvillous Structures of Rat Olfactory and Nasal Respiratory Epithelia—A Study Using Ultra-Rapid Cryo-Fixation Followed by Freeze-Substitution or Freeze-Etching. *Cell Tissue Res.* **1984**, *235*, 225–241. [CrossRef] [PubMed]
262. Chandler, D.; Heuser, J. Membrane Fusion during Secretion: Cortical Granule Exocytosis in Sex Urchin Eggs as Studied by Quick-Freezing and Freeze-Fracture. *J. Cell Biol.* **1979**, *83*, 91. [CrossRef]
263. Chandler, D.; Heuser, J. Arrest of Membrane Fusion Events in Mast Cells by Quick-Freezing. *J. Cell Biol.* **1980**, *86*, 666. [CrossRef] [PubMed]
264. Ornberg, R.; Reese, T. Beginning of Exocytosis Captured by Rapid-Freezing of Limulus Amebocytes. *J. Cell Biol.* **1981**, *90*, 40. [CrossRef]
265. Chandler, D. Comparison of Quick-Frozen and Chemically Fixed Sea-Urchin Eggs: Structural Evidence That Cortical Granule Exocytosis Is Preceded by a Local Increase in Membrane. *J. Cell Sci.* **1984**, *72*, 23–36. [CrossRef]

266. Wagner, R.; Andrews, S. Ultrastructure of the Vesicular System in Rapidly Frozen Capillary Endothelium of the Rete Mirabile. *J. Ultrastruct. Res.* **1985**, *90*, 172–182. [CrossRef]
267. Plattner, H.; Bachmann, L. Cryofixation: A Tool in Biological Ultrastructural Research. *Elsevier* **1982**, *79*, 237–304.
268. Christensen, A.K. Frozen Thin Sections of Fresh Tissue for Electron Microscopy, with a Description of Pancreas and Liver. *J. Cell Biol.* **1971**, *51*, 772–804. [CrossRef] [PubMed]
269. Dempsey, G.P.; Bullivant, S. A Copper Block Method for Freezing Non-cryoprotected Tissue to Produce Ice-crystal-free Regions for Electron Microscopy: I. Evaluation Using Freeze-substitution. *J. Microsc.* **1976**, *106*, 251–260. [CrossRef]
270. Eränkö, O. Quenching of Tissues for Freeze-Drying. *Cells Tissues Organs* **1954**, *22*, 331–336. [CrossRef]
271. Wollenberger, A.; Ristau, O.; Schoffa, G. Eine Einfache Technik Der Extrem Schnellen Abkühlung Größerer Gewebestücke. *Pflügers Arch. Für Die Gesamte Physiol. Des Menschen Und Der Tiere* **1960**, *270*, 399–412. [CrossRef]
272. Sjöström, M.; Cytochemistry, R.J. *Cryo-Ultramicrotomy of Muscles in Defined State. Methodological Aspects*; North-Holland Publishing Company: Amsterdam, The Netherlands, 1974.
273. Moor, H. Recent Progress in the Freeze-Etching Technique. *Philos. Trans. R. Soc. Lond. B Biol. Sci.* **1971**, *261*, 121–131. [CrossRef]
274. Moor, H.; Bellin, G.; Sandri, C.; Akert, K. The Influence of High Pressure Freezing on Mammalian Nerve Tissue. *Cell Tissue Res.* **1980**, *209*, 201–216. [CrossRef]
275. Hunziker, E.B.; Herrmann, W.; Schenk, R.K.; Mueller, M.; Moor, H. Cartilage Ultrastructure after High Pressure Freezing, Freeze Substition, and Low Temperature Embedding. I. Chondrocyte Ultrastructure—Implications for the Theories of Mineralization and Vascular Invasion. *J. Cell Biol.* **1984**, *98*, 267–276. [CrossRef]
276. Marti, R.; Wild, P.; Schraner, E.M.; Mueller, M.; Moor, H. Parathyroid Ultrastructure after Aldehyde Fixation, High-Pressure Freezing, or Microwave Irradiation. *J. Histochem. Cytochem.* **1987**, *35*, 1415–1424. [CrossRef]
277. Wolf, K.V.; Stockem, W.; Wohlfarth-Bottermann, K.E.; Moor, H. Cytoplasmic Actomyosin Fibrils after Preservation with High Pressure Freezing. *Cell Tissue Res.* **1981**, *217*, 479–495. [CrossRef]
278. Wan, L.; Powell-Palm, M.; Lee, C.; Gupta, A.; Weegman, B.; Clemens, M.; Rubinsky, B. Preservation of Rat Hearts in Subfreezing Temperature Isochoric Conditions to—8 C and 78 MPa. *Biochem. Biophys. Res. Commun.* **2018**, *496*, 852–857. [CrossRef]
279. Năstase, G.; Lyu, C.; Ukpai, G.; Şerban, A.; Rubinsky, B. Isochoric and Isobaric Freezing of Fish Muscle. *Biochem. Biophys. Res. Commun.* **2017**, *485*, 279–283. [CrossRef] [PubMed]
280. Preciado, J.; Rubinsky, B. The Effect of Isochoric Freezing on Mammalian Cells in an Extracellular Phosphate Buffered Solution. *Cryobiology* **2018**, *82*, 155–158. [CrossRef] [PubMed]
281. Pauli, B.U.; Weinstein, R.S.; Soble, L.W.; Alroy, J. Freeze Fracture of Monolayer Cultures. *J. Cell Biol.* **1977**, *72*, 763–769. [CrossRef] [PubMed]
282. Saritha, K.R.; Bongso, A. Comparative Evaluation of Fresh and Washed Human Sperm Cryopreserved in Vapor and Liquid Phases of Liquid Nitrogen. *J. Androl.* **2001**, *22*, 857–862. [CrossRef]
283. Chang, H.J.; Lee, J.R.; Chae, S.J.; Jee, B.C.; Suh, C.S.; Kim, S.H. Comparative Study of Two Cryopreservation Methods of Human Spermatozoa: Vitrification versus Slow Freezing. *Fertil. Steril.* **2008**, *90*, S280. [CrossRef]
284. Deng, X.; Hua, Z.; Xuan, Y.; Hongling, Y.; Chengmei, Z.; Lan, C.; Ruichang, L.; Wenjun, L. Cryopreserved Ovarian Tissues Can Maintain a Long-Term Function after Heterotopic Autotransplantation in Rat. *Reproduction* **2009**, *138*, 519–525. [CrossRef]
285. Lee, J.; Kim, E.J.; Kong, H.S.; Youm, H.W.; Kim, S.K.; Lee, J.R.; Suh, C.S.; Kim, S.H. Establishment of an Improved Vitrification Protocol by Combinations of Vitrification Medium for Isolated Mouse Ovarian Follicles. *Theriogenology* **2018**, *121*, 97–103. [CrossRef]
286. Ramezani, M.; Salehnia, M.; Jafarabadi, M. Short Term Culture of Vitrified Human Ovarian Cortical Tissue to Assess the Cryopreservation Outcome: Molecular and Morphological Analysis. *J. Reprod. Infertil.* **2017**, *18*, 162.
287. Murray, P.W.L.R.; Robards, A.W.; Waites, P.R. Countercurrent Plunge Cooling: A New Approach to Increase Reproducibility in the Quick Freezing of Biological Tissue. *J. Microsc.* **1989**, *156*, 173–182. [CrossRef]
288. Bridgman, P.C.; Reese, T.S. The Structure of Cytoplasm in Directly Frozen Cultured Cells. I. Filamentous Meshworks and the Cytoplasmic Ground Substance. *J. Cell Biol.* **1984**, *99*, 1655–1668. [CrossRef]
289. FEDER, N.; SIDMAN, R.L. Methods and Principles of Fixation by Freeze-Substitution. *J. Biophys. Biochem. Cytol.* **1958**, *4*, 593–600. [CrossRef]
290. Paul, A.K.; Liang, Y.; Srirattana, K.; Nagai, T.; Parnpai, R. Vitrification of Bovine Matured Oocytes and Blastocysts in a Paper Container. *Anim. Sci. J.* **2018**, *89*, 307–315. [CrossRef] [PubMed]
291. Arav, A.; Natan, Y.; Kalo, D.; Komsky-Elbaz, A.; Roth, Z.; Levi-Setti, P.E.; Leong, M.; Patrizio, P. A New, Simple, Automatic Vitrification Device: Preliminary Results with Murine and Bovine Oocytes and Embryos. *J. Assist. Reprod. Genet.* **2018**, *35*, 1161–1168. [CrossRef] [PubMed]
292. Olexiková, L.; Makarevich, A.V.; Bédeová, L.; Kubovičová, E. The Technique for Cryopreservation of Cattle Eggs. *Slovak J. Anim. Sci.* **2019**, *52*, 166–170.
293. Bachmann, L.; Schmitt, W.W. Improved Cryofixation Applicable to Freeze Etching (Spray-Freezing/Solute Model Systems/Liquid Nitrogen and Propane). 1971. Volume 68. Available online: https://www.pnas.org/content/68/9/2149.short (accessed on 19 May 2020).

294. Knoll, G.; Braun, C.; Plattner, H. Quenched Flow Analysis of Exocytosis in Paramecium Cells: Time Course, Changes in Membrane Structure, and Calcium Requirements Revealed after Rapid Mixing and Rapid Freezing of Intact Cells. *J. Cell Biol.* **1991**, *113*, 1295–1304. [CrossRef]
295. De Vries, R.J.; Banik, P.D.; Nagpal, S.; Weng, L.; Ozer, S.; Van Gulik, T.M.; Toner, M.; Tessier, S.N.; Uygun, K. Bulk Droplet Vitrification: An Approach to Improve Large-Scale Hepatocyte Cryopreservation Outcome. *Langmuir* **2019**, *35*, 7354–7363. [CrossRef]
296. Dou, R.; Saunders, R.; Mohamet, L.; Ward, C.; Chip, B.D.-L. on a; 2015, undefined. High Throughput Cryopreservation of Cells by Rapid Freezing of Sub-Ml Drops Using Inkjet Printing–Cryoprinting. *Lab a Chip* **2015**, *15*, 3503–3513. [CrossRef] [PubMed]
297. Plattner, H.; Artalejo, A.R.; Neher, E. Ultrastructural Organization of Bovine Chromaffin Cell Cortex—Analysis by Cryofixation and Morphometry of Aspects Pertinent to Exocytosis. *J. Cell Biol.* **1997**, *139*, 1709–1717. [CrossRef]
298. Espevik, T.; Elgsaeter, A. In Situ Liquid Propane Jet-Freezing and Freeze-Etching of Monolayer Cell Cultures. *J. Microsc.* **1981**, *123*, 105–110. [CrossRef]
299. Katkov, I.I.; Bolyukh, V.F.; Sukhikh, G.T. KrioBlast TM as a New Technology of Ultrafast Cryopreservation of Cells and Tissues. 2. Kinetic Vitrification of Human Pluripotent Stem Cells and Spermatozoa. *Bull. Exp. Biol. Med.* **2018**, *165*, 63–68. [CrossRef]
300. Bolyukh, V.F.; Katkov, I.I.; Bolyukh, V.F. KRIOBLAST ^{TM}: A PROMISING CRYOGENIC PLATFORM FOR KINETIC VITRIFICATION BY HYPERFATST COOLING. In Proceedings of the 2nd Thermal and Fluid Engineering Conference, TFEC2017, 4th International Workshop on Heat Transfer, IWHT2017, Las Vegas, NV, USA, 2–5 April 2017.
301. Patra, T.; Gupta, M.K. Solid Surface Vitrification of Goat Testicular Cell Suspension Enriched for Spermatogonial Stem Cells. *Cryobiology* **2022**, *104*, 8–14. [CrossRef] [PubMed]
302. Patra, T.; Gupta, M.K. Cryopreservation of Murine Testicular Leydig Cells by Modified Solid Surface Vitrification with Supplementation of Antioxidants. *Cryobiology* **2019**, *88*, 38–46. [CrossRef] [PubMed]
303. Brito, D.C.C.; Domingues, S.F.S.; Rodrigues, A.P.R.; Figueiredo, J.R.; Santos, R.R.; Pieczarka, J.C. Vitrification of Domestic Cat (Felis Catus) Ovarian Tissue: Effects of Three Different Sugars. *Cryobiology* **2018**, *83*, 97–99. [CrossRef] [PubMed]
304. Rodriguez Villamil, P.; Lozano, D.; Oviedo, J.M.; Ongaratto, F.L.; Bó, G.A. Developmental Rates of in Vivo and in Vitro Produced Bovine Embryos Cryopreserved in Ethylene Glycol Based Solutions by Slow Freezing or Solid Surface Vitrification. *Anim. Reprod.* **2012**, *9*, 86–92.
305. Sharma, A.; Bischof, J.C.; Finger, E.B. Liver Cryopreservation for Regenerative Medicine Applications. *Regen. Eng. Transl. Med.* **2021**, *7*, 57–65. [CrossRef]
306. Manuchehrabadi, N.; Gao, Z.; Zhang, J.; Ring, H.L.; Shao, Q.; Liu, F.; McDermott, M.; Fok, A.; Rabin, Y.; Brockbank, K.G.M. Improved Tissue Cryopreservation Using Inductive Heating of Magnetic Nanoparticles. *Sci. Transl. Med.* **2017**, *9*, eaah4586. [CrossRef]
307. Khosla, K.; Zhan, L.; Bhati, A.; Carley-Clopton, A.; Hagedorn, M.; Bischof, J. Characterization of Laser Gold Nanowarming: A Platform for Millimeter-Scale Cryopreservation. *Langmuir* **2019**, *35*, 7364–7375. [CrossRef]
308. Ruan, H.; Wang, T.; Gao, C. Microwave-Water Bath Hybrid Warming for Frozen Cryoprotectant Solution Using a Helical Antenna. *Cryoletters* **2020**, *41*, 26–30.
309. Zhan, L.; Han, Z.; Shao, Q.; Etheridge, M.L.; Hays, T.; Bischof, J.C. Rapid Joule Heating Improves Vitrification Based Cryopreservation. *Nat. Commun.* **2022**, *13*, 1–15. [CrossRef]
310. Giwa, S.; Lewis, J.K.; Alvarez, L.; Langer, R.; Roth, A.E.; Church, G.M.; Markmann, J.F.; Sachs, D.H.; Chandraker, A.; Wertheim, J.A. The Promise of Organ and Tissue Preservation to Transform Medicine. *Nat. Biotechnol* **2017**, *35*, 530–542. [CrossRef]

Disclaimer/Publisher's Note: The statements, opinions and data contained in all publications are solely those of the individual author(s) and contributor(s) and not of MDPI and/or the editor(s). MDPI and/or the editor(s) disclaim responsibility for any injury to people or property resulting from any ideas, methods, instructions or products referred to in the content.